Journal of Iberian Geology
https://doi.org/10.1007/s41513-020-00135-y

RESEARCH PAPER

A late Permian ichthyofauna from the Zechstein Basin, Lithuanian–Latvian Region

Darja Dankina[1] · Andrej Spiridonov[1] · Ģirts Stinkulis[2] · Esther Manzanares[3] · Sigitas Radzevičius[1]

Received: 10 March 2020 / Accepted: 8 August 2020

Abstract

The late Permian was a transformative time, which ended with one of the most significant extinction events in Earth's history. Fish assemblages are a major component of marine food webs. The macroevolution and biogeographic patterns of late Permian fish are currently insufficiently known. In this contribution, a late Permian ichthyofauna from the Kūmas quarry (southern Latvia) is described for the first time. The studied late Permian Latvian assemblage consisted of isolated chondrichthyan teeth putatively associated to ? *Helodus* sp., ?*Acrodus* sp., ? *Omanoselache* sp. and euselachian-type dermal denticles as well as many actinopterygian scales, numerous teeth and multiple unidentifiable microremains. This ichthyofaunal assemblage is very similar to the contemporaneous Lopingian complex of the Naujoji Akmenė formation from the Karpėnai quarry (northern Lithuania), despite the fact that the Kūmas assemblage is more diverse and abundant, in terms of fossil remains. The differences in the abundance of microremains could possibly be explained by a fresh water influx into the north-eastern Zechstein Basin margin, which probably reduced the salinity of the sea water. The new data enable a better understanding of the poorly known late Permian fish diversity from the north–eastern part of the basin.

Keywords Microremains · Chondrichthyans · Actinopterygians · Histology · Permian · Baltic

Resumen

El Pérmico superior fue un periodo transformador, que terminó con una de las extinciones más masivas de la historia de la Tierra. Los peces son un componente importante de las redes tróficas marinas. Los patrones macroevolutivos y biogeográficos de los peces del Pérmico superior han sido escasamente estudiados. En este trabajo describimos por primera vez la ictiofauna de la cantera de Kūmas (sur de Letonia). La asociación estudiada consiste en dientes de condrictios aislados asociados a ?*Helodus* sp., ? *Acrodus* sp., ? *Omanoselache* sp.; escamas de tipo Euselachii y de actinopterigios; numerosos dientes y otros microrestos no identificables. La asociación de ictiofauna descrita es muy similar a la actual del complejo

✉ Darja Dankina
darja.dankina@gmail.com

Andrej Spiridonov
s.andrej@gmail.com

Ģirts Stinkulis
girts.Stinkulis@lu.lv

Esther Manzanares
esther.manzanares@uv.es

Sigitas Radzevičius
sigitas.radzevicius@gf.vu.lt

[1] Department of Geology and Mineralogy, Vilnius University, Vilnius, Lithuania

[2] Faculty of Geography and Earth Sciences, University of Latvia, Riga, Latvia

[3] Department of Botany and Geology, University of Valencia, Valencia, Spain

Published online: 26 September 2020

Lopingian de la formación Naujoji Akmenė de la cantera Karpėnai (norte de Lituania), aunque la asociación de Kūmas es más diversa y abundante en términos numéricos. Las diferencias de abundancia de microrestos puede ser debido a un aporte de agua dulce en el margen noroeste de la cuenca Zechstein que probablemente hizo disminuir la salinidad del agua de mar. Estos nuevos datos permiten entender más profundamente la diversidad del registro escasamente conocido del Pérmico superior del noroeste de la cuenca.

Keywords Microrestos · Condrictios · Actinopterigios · Histología · Pérmico · Báltico.

1 Introduction

The Lopingian is currently one of the most studied time periods from the Phanerozoic, as it is characterized by two phases of the end-Permian mass extinction, which significantly affected long-term macroevolution (Wignall 2015). Despite an overall low level of the detailed taxonomic palaeoichthyological analysis, there is increased interest in the late Permian fish assemblages, which are mostly composed of isolated chondrichthyan and osteichthyan remains (dermal denticles, scales, fin spines, vertebral centra, teeth), thus demonstrating their usefulness for palaeoenvironmental and palaeoecological reconstructions of marine vertebrate from the time period immediately preceding the Permian–Triassic mass extinction (Koot 2013; Romano et al. 2016).

Osteichthyans and chondrichthyans represent the dominant fish classes among marine and freshwater vertebrates since the Carboniferous period (Romano et al. 2016; Sallan and Coates 2010), and are relatively common in the late Permian fossil records worldwide including Europe. Late Permian fish fossils were found and described in Germany (Diedrich 2009), England (King 1850), eastern Greenland (Nielsen 1952), Poland (Kazmierczak 1967) and Lithuania (Dankina et al. 2017).

The late Permian Zechstein Basin is a marine and partly evaporitic intracratonic basin (Sørensen et al. 2007) which formed when the Boreal Ocean broke in from the north, thus immediately forming an almost enclosed sea (Smith 1979) (Fig. 1). The sea extends from England through northern Germany into Poland and the south Latvia (Van Wees et al. 2000).

The current study represents the first record of a fish assemblage from the southern Latvia which was the north-easternmost part of the Zechstein Basin. The numerous remains (euselachian-type dermal denticles, chondrichthyan teeth, actinopterygian scales and teeth) have little taxonomic significance and rather low comparative material. For these reasons, we divided remains into various morphotypes according to their morphological differences. The material was also compared to the late Permian material which was earlier found in the northern Lithuania (Dankina et al. 2017). We present computed tomographic and histologic models of the internal vascular structures of the isolated vertebrate fossils from the both localities. This new fossil fish assemblage will provide a better understanding of late Permian palaeobiogeography and palaeoecology, and the fish migration in the Zechstein Basin.

2 Geological settings

The Southern Permian Basin (Zechstein) extends over a distance of 1700 km from England across the Southern North Sea through northern Germany into Poland and the south Latvia (Van Wees et al. 2000) (Fig. 1a). Latvia is located in the north-easternmost part of Zechstein Basin (Raczyński and Biernacka 2014) (Fig. 1b).

The Naujoji Akmenė Formation is exposed in the south Latvia (Raczyński and Biernacka 2014). This Formation is represented here by five members: Auce, Sātiņi, Kūmas, Alši, and Pampāļi (Kuršs and Savvaitova 1986; Gailīte et al. 2000; Lukševičs et al. 2012). The Auce Member is composed of clayey limestone and distributed only in the eastern part of the Wuchiapingian, late Permian distribution area in Latvia. Clay admixture likely is due to rewashing of the underlying clayey Famennian deposits during the beginning of the Permian sedimentation (Kuršs and Savvaitova 1986). The Sātiņi Member is represented by sandy limestone and sand with quite abundant bivalve fossils. This member is present in the central and western part of the late Permian distribution area in Latvia (Kuršs and Stinkule 1997). The sand admixture likely is due to the underlying sandy Famennian and Carboniferous deposits (Kuršs and Savvaitova 1986). The Kūmas and Alši members are present in all territory of the late Permian distribution area of Latvia. The Kūmas Member is composed of earthy limestone with interlayers and nodules ("loafs") of cryptocrystalline porcelain-like limestone. It is followed by the Alši Member, which is made of biodetrital and skeletal limestone with bivalves, brachiopods, and foraminifera. The upper one of the late Permian succession in Latvia, the Pampāļi Member, is present in southern and south-western parts of the late Permian distribution area in Latvia. The Pampāļi Member is composed of dolomitized limestone and ooidal dolostone (Kuršs and Savvaitova 1986; Gailīte et al. 2000). The total thickness of the Permian differs from 30–145 m on the western side

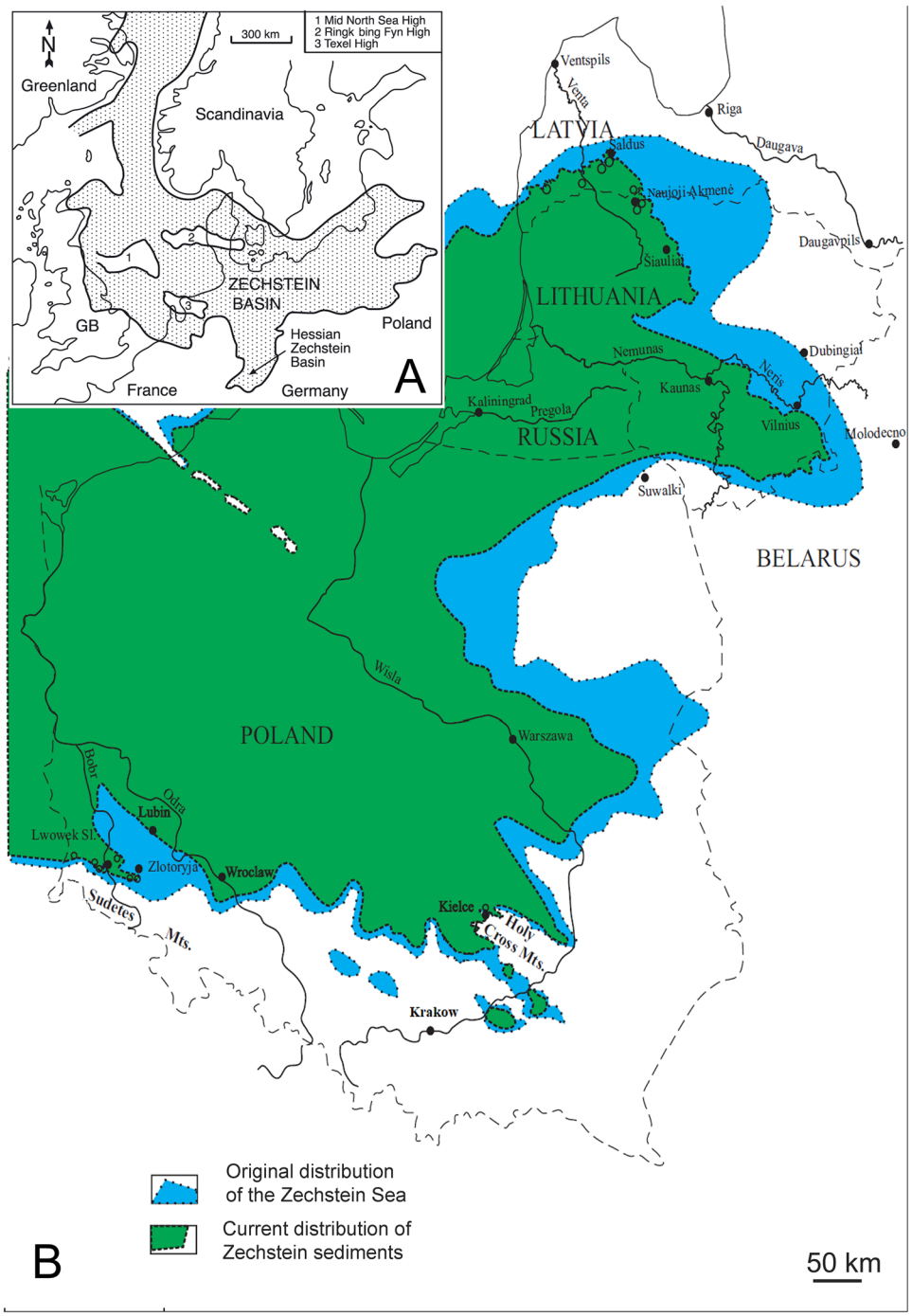

Fig. 1 **a** Palaeogeography of the European Zechstein Basin (modified after Becker and Bechstädt 2006). **b** Geographical position of the Kūmas and Karpėnai quarries (modified after Raczyński and Biernacka 2014)

of the river Venta to the 20–40 m on the eastern side of the river Venta and less than 20 m in the north and east part of late Permian distribution in Latvia (Kuršs and Savvaitova 1986) (Fig. 2).

3 Material and methods

Samples were collected in the Kūmas quarry, southern Latvia (56° 34′56″ N; 22° 35′82″ E). One sample was collected from Satini/Auce Member; five samples from Kūmas Member and five samples from Alši Member. The total weight of the 11 collected samples from the Kūmas quarry reached ~ 220 kg. Collected samples are yielded 2164 isolated fish microremains (Table 1).

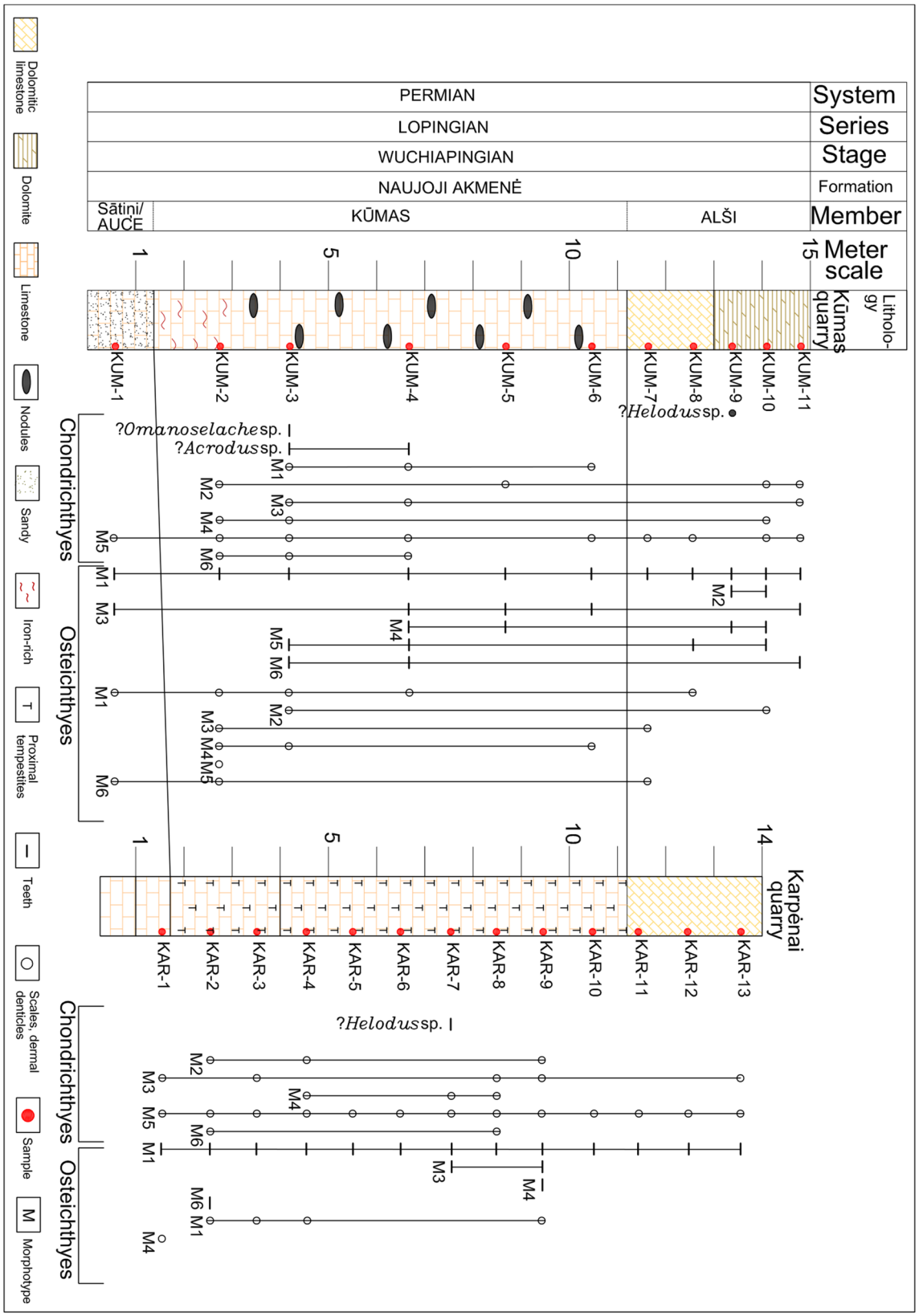

Fig. 2 Stratigraphical profile of the Kūmas quarry (southern Latvia) and Karpėnai quarry (northern Lithuania) with an indication of the late Permian fish assemblage, and a stratigraphic repartition of the chondrichthyan and osteichthyan taxa based on isolated teeth, dermal denticles and scales

Table 1 Abundance of palaeoichthyofaunal microremains from the Kūmas quarry

Sample	Height, m	Chondrichthyan							Actinopterygian											
		Tooth	Scale						Tooth						Scale					
			M1	M2	M3	M4	M5	M6	M1	M2	M3	M4	M5	M6	M1	M2	M3	M4	M5	M6
KUM-11	14.0–15.0			2	2		60		211		3			1						
KUM-10	13.0–14.0			2		1	1		12	1		2	2			1				
KUM-9	12.5–13.0	1							21	1		1								
KUM-8	12.0–12.5						1		3				1		1					
KUM-7	11.5–12.0						2		6								1			2
KUM-6	10.5–11.5		1				1		15		1							1		
KUM-5	7.5–10.5			1					29		1	1								
KUM-4	5.0–7.5	3	1		1		73	1	212		2	3	1	2	35					
KUM-3	2.5–5.0	13	2		2	2	72	1	937				1	1	102	3		4		
KUM-2	0.5–2.5			1		1	11	1	209						44		3	5	4	1
KUM-1	0.0–0.5						2		12		1				4					1
Total:	**15.0**	**17**	**4**	**6**	**5**	**4**	**223**	**3**	**1667**	**2**	**8**	**7**	**5**	**4**	**186**	**4**	**4**	**10**	**4**	**4**

The fossils were chemically extracted from the samples using etching technique described by Jeppsson et al. (1999). In a vessel were mixed a 23.3 l of 60% acetic acid and 116.7 l of the tap water. The vessel left for over 48 h. The residue was dried in the room temperature and sieved from 0.2 to 0.063 mm to extract tiny remains into microslides. A selected number of the isolated fish elements were photographed using a HITACHI S4800-FEG scanning electron microscope (SEM) at the University of Valencia (Valencia, Spain) and a FEI Quanta 250 SEM at the Nature Research Centre (Vilnius, Lithuania).

To analyse the presence of enameloid layer in the late Permian fish teeth and dermal denticles polished sections were prepared. Teeth and dermal denticles were embedded in a transparent polyester resin at 120 °C for 30–45 min prior to polishing with a carborundum (1200 µm) until the desired part of the fossil was reached. After that, the sections were etched for 5–10 s in 10% HCl acid to elucidate the enameloid microstructure. The prepared polished fossils were coating with a gold–palladium alloy prior to photographing with the Hitachi S4800-FEG SEM at the Microscope Service at the University of Valencia. The polished sections technique used here has been described by Manzanares et al. (2014).

?*Helodus* tooth and euselachian dermal denticle were scanned at a Synchrotron Light Source from the Paul Scherrer Institute (PSI) in Zurich, Switzerland. The vascularization system of the analysed fossils was reconstructed using Avizo 8.1 software at the University of Valencia. The software was utilised to perform 3D model of the fossils and the transparent mode of any tissues which used for the reconstruction of canal system.

All the material presented here is stored in the Geological Museum at the Institute of Geosciences of Vilnius University.

4 Systematic palaeontology

Class CHONDRICHTHYES Huxley (1880)
Subclass ELASMOBRANCHII Bonaparte (1832)
Order HYBODONTIFORMES Patterson (1966)
Family ACRODONTIDAE Casier (1959)
Genus *ACRODUS* Agassiz (1838)
?ACRODUS sp.
(Fig. 3 a, b)

Material

Fifteen isolated teeth, of which only two with preserved roots, were found in the Kūmas quarry in southern Latvia. This genus is represented and described here by a tooth without a root [VU-ICH-KUM-001] and one with a preserved root [VU-ICH-KUM-002].

Description

The teeth crown has a convex elliptical shape, with a well-developed sculptured surface made of the coarse, anastomosing ridges originating (Fig. 3A1). It reaches 0.2 mm in mesio-distal and 0.05 mm in labio-lingual. The flat basal plate displays the same outline as the crown; the preserved roots have numerous canal openings in the proximal view (Fig. 3B), although, most of the roots are absent (Fig. 3A2).

Remarks

The hybodontoid teeth have been putatively assigned to *Acrodus* sp. teeth. Morphological similarities of the crown (crown shape and ornament) can be detected in an *Acrodus*

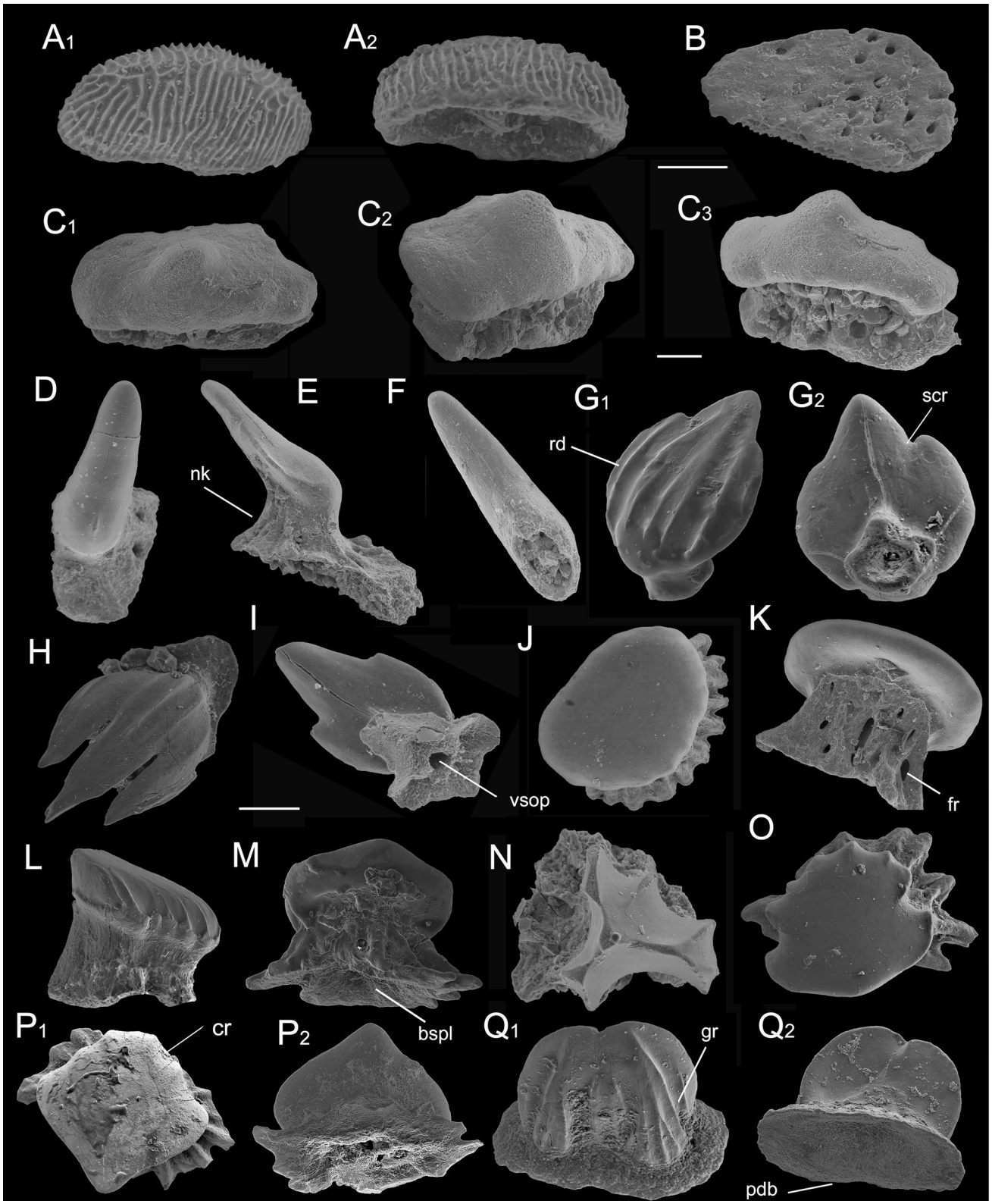

kalasinensis tooth from the Late Jurassic-Early Cretaceous from north-eastern Thailand (Cuny et al. 2014) and an *Acrodus spitzbergensis* teeth from the Lower Triassic of Spitsbergen (Błażejowski 2004). Also, similar crown morphology was found and described as *Acrodus* sp. tooth [P.12151] from the Upper Permian in the Punjab, India (these specimens are deposited in the Natural History Museum in London, UK). The main difference between comparative material is absent

◂**Fig. 3** SEM images of the late Permian chondrichthyan dermal denticles, *?Acrodus* sp. and ?*Omanoselache* sp. teeth from the Kūmas quarry. **A** *?Acrodus* sp. tooth, VU-ICH-KUM-001 from the KUM-3 sample; $\mathbf{A_1}$ tooth in occlusal view; $\mathbf{A_2}$ in oblique lateral view. **B** VU-ICH-KUM-002 from the KUM-3 sample in basal view. **C** *?Omanoselache* sp. tooth, VU-ICH-KUM-003 from the KUM-3 sample; $\mathbf{C_1}$ tooth in occlusal view; $\mathbf{C_2}$ in oblique occlusal view; $\mathbf{C_3}$ in lateral view. **D–F** Morphotype 1. **D** VU-ICH-KUM-004 in occlusal view from the KUM-4 sample. **E** VU-ICH-KUM-005 in lateral view from the KUM-3 sample. **F** VU-ICH-KUM-006 in subcrown view from the KUM-3 sample. **G–I** Morphotype 2. **G** VU-ICH-KUM-007 from the KUM-2 sample; $\mathbf{G_1}$ in occlusal view; $\mathbf{G_2}$ in basal view. **H** VU-ICH-KUM-008 in occlusal view from the KUM-10 sample. **I** VU-ICH-KUM-09 in basal view from the KUM-10 sample. **J–M** Morphotype 3. **J** VU-ICH-KUM-010 in occlusal view from the KUM-3 sample. **K** VU-ICH-KUM-011 in lateral view from the KUM-3 sample. **L** VU-ICH-KUM-012 in lateral view from the KUM-11 sample. **M** VU-ICH-KUM-013 in lateral view from the KUM-2 sample. **N** Morphotype 4. **N** VU-ICH-KUM-014 in occlusal view from the KUM-10 sample. **O**, **P** Morphotype 5. **O** VU-ICH-KUM-015 in occlusal view from the KUM-2 sample. **P** VU-ICH-KUM-016 from the KUM-2 sample. $\mathbf{P_1}$ in occlusal view; $\mathbf{P_2}$ in oblique basal view. **Q** Morphotype 6. **Q** VU-ICH-KUM-017 from the KUM-2 sample; $\mathbf{Q_1}$ in occlusal view; $\mathbf{Q_2}$ in oblique basal view. *bspl* basal plate, *cr* crown, *fr* foramina, *gr* grooves, *nk* neck, *pdb* pedicle base, *rd* ridges, *scr* subcrown, *vsop* vascular opening. The scale bars equal 0.1 mm, respectively

of the distinct mesial juncture in the centre of the crown, which is clearly shown for example in *Acrodus* sp. teeth from Early Permian of Texas (Johnson 1981). Moreover, according to the Ginter (2010) only several *Acrodus* sp. occurrences are known from Palaeozoic which assigned to Upper Pennsylvanian and Lower Permian of USA (Johnson 1981).

INCERTAE FAMILIAE

Genus *OMANOSELACHE* Koot et al. (2013)

?OMANOSELACHE sp.

(Fig. 3C)

Material

Isolated tooth [VU-ICH-KUM-003] from the Kūmas quarry in southern Latvia.

Description

The shape of the crown is robust, elongated and generally smooth; it has a flattened appearance. The crown's surface is slightly but clearly asymmetrical (Fig. 3C1); it reaches 0.7 mm mesio-distally, 0.3 mm labio-lingually and is around 0.35–0.4 mm high. The central transverse part of the crown is convex and has a single small, blunt cusp located on the labial margin (Fig. 3C2). The neck is massive and broad, with some canal openings filled with sediment (Fig. 3C3). The basal plate is elliptical in shape, reaching 0.7 mm in length and 0.3 mm in width.

Remarks

Similar morphological features as asymmetrical crown and its smooth surface with rounded, blunt apex of the moderate main cusp, the small labial intended peg, and the base with randomly located foramina were found in an elongate tooth three times bigger in size from the Knuff Formation of the Middle Permian in Oman (Koot et al. 2013).

Cohort EUSELACHII Hay (1902)

EUSELACHII indet

(Fig. 3D–Q).

Material

Two hundred and forty five isolated chondrichthyan dermal denticles were found in the Kūmas quarry in southern Latvia and 113 denticles in the Karpėnai quarry in northern Lithuania. These denticles were classified into six morphotypes based on their morphological features and are represented here to 14 dermal denticles [VU-KUM-ICH-004—VU-KUM-ICH-017].

Description

Well-preserved fossils are identified as euselachian-type dermal denticles based on resembling material from the Upper Carboniferous in the western Argentina (Saravia 2001); from the Upper Jurassic in Tanzania (Arratia et al. 2002); from the Middle and Late Triassic in north-eastern British Columbia, Canada (Johns 1996); from the Middle Permian in the Apache Mountains, West Texas (USA) (Ivanov et al. 2013); and are divided into morphotypes based on morphological differences between their crowns, necks and base profile.

Morphotype 1

Four microremains from this morphotype were found in the Kūmas quarry (Fig. 3D–F). The crown is blunt, shaped like a horn, elongated, slightly compressed in lateral view and smooth: it has a high neck and a wide base (Fig. 3D–E). The crown and base lengths are similar—around 0.5–0.6 mm—but the directions of growth are opposite (Fig. 3E). The crown is slightly narrower than the neck – 0.2 mm. The pedicle base is sometimes absent (Fig. 3F) or has some foramina in the vascular system, which are usually filled with sediment.

Morphotype 2

Six dermal denticles were found in the Kūmas quarry and 15 denticles in Karpėnai quarry. They have a trident or nearly trident crown with a low, slender and narrow neck, hidden under the crown in apical view (Fig. 3G1, H). The exterior

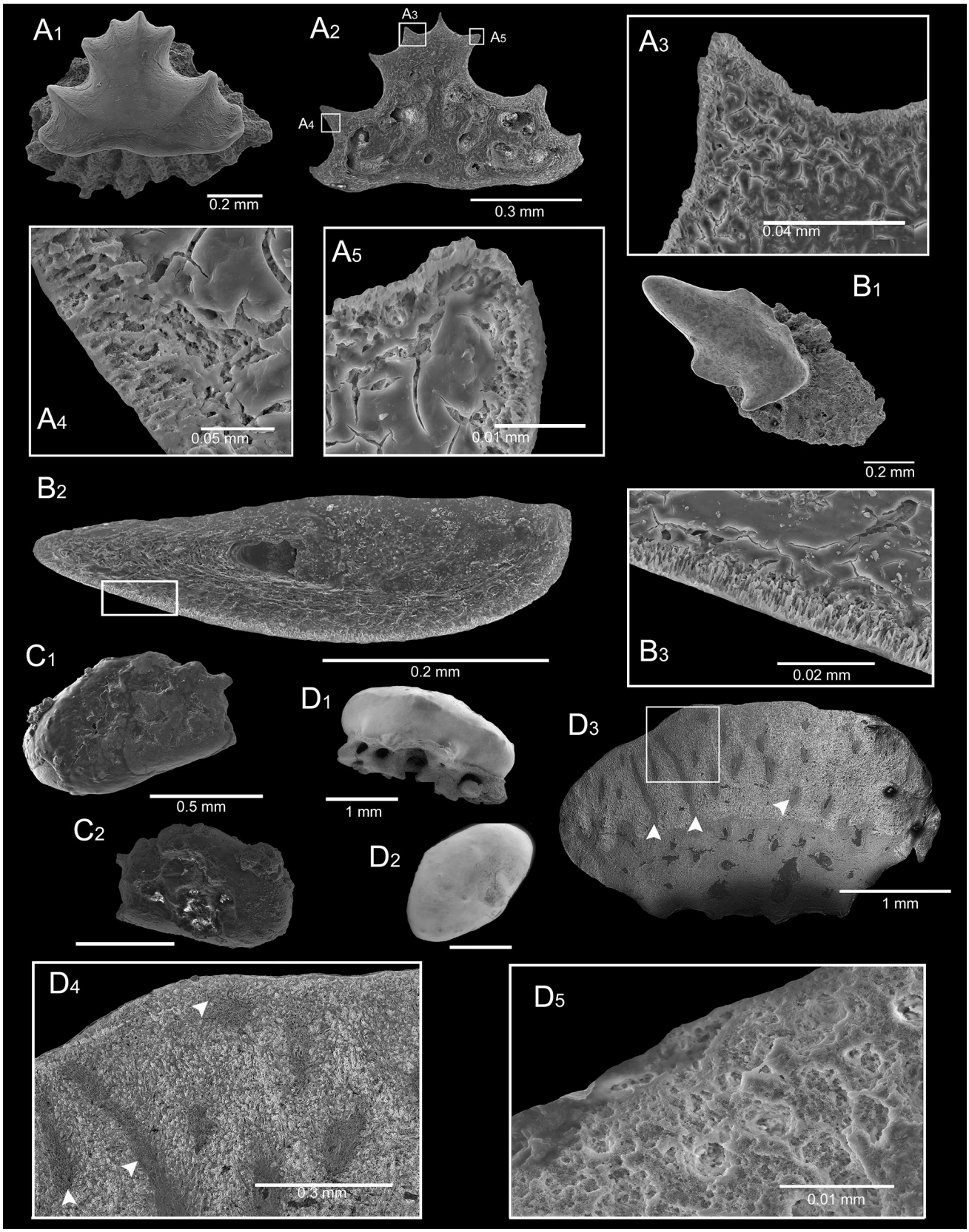
A1
0.2 mm
A2
A3
A5
A4
0.3 mm
A3
0.04 mm
A4
0.05 mm
A5
0.01 mm
B1
0.2 mm
B2
0.2 mm
B3
0.02 mm
C1
0.5 mm
C2
D1
1 mm
D2
D3
1 mm
D4
0.3 mm
D5
0.01 mm

◂**Fig. 4** The histology of the euselachian-type dermal denticles and ?*Helodus* sp. tooth [VU-ICH-KAR-012] from the Karpėnai quarry and ?*Helodus* sp. tooth from Kūmas quarry. **A** VU-ICH-KAR-014 from the KAR-7 sample. $\mathbf{A_1}$ General view of the dermal denticle; $\mathbf{A_2}$ general view of the longitudinal section of the denticle; $\mathbf{A_3}$–$\mathbf{A_5}$ enameloid covering the top surface of the crown. **B** VU-ICH-KAR-016 from the KAR-11 sample. $\mathbf{B_1}$ General view of the dermal denticle; $\mathbf{B_2}$ general view of the longitudinal section of the denticle; $\mathbf{B_3}$ enameloid covering the top surface of the crown. **C** VU-ICH-KUM-018 from the KUM-9 sample. $\mathbf{C_1}$ The poorly preserved fossil in occlusal view; $\mathbf{C_2}$ in basal view. $\mathbf{D_1}$ The entire isolated fossil in lateral view; $\mathbf{D_2}$ in occlusal view; $\mathbf{D_3}$ the longitudinal sectioned tooth with a well-differentiated cap of enameloid and a distinct enameloid-dentine junction (EDJ); $\mathbf{D_4}$ in visual detail, the penetrating canals of the enameloid layer indicated by the white arrow pointers; $\mathbf{D_5}$ in visual detail, some randomly arranged enameloid crystallites. The white rectangles represent the outer layer of the crown in detail

of the crown is sculptured with some (usually five) gentle convex ridges and furrows originating from the longitudinal crest and reaching 0.3–0.4 mm length. The crown sits horizontally or slightly obliquely up on the neck. The base has a rhomboid surface and one roundish canal opening in proximal view (Fig. 3G2, I). The denticle reaches 0.3–0.4 mm height and 0.4–0.5 mm crowns length/width.

Morphotype 3

Five roundish or semi-roundish dermal denticles were found in the Kūmas quarry and seven denticles in Karpėnai quarry. This type of denticles have a slightly elongated blunt cusp in the posterior margin of the crown (Fig. 3J–M). The crown surface is thick, without ornamentation, or covered with some short convex ridges and furrows on the anterior side (Fig. 3J, L). The crown sits horizontally or slightly obliquely up on the neck (Fig. 3L) and reaches around 0.4–0.8 mm in diameter. The neck is relatively high, massive and has numerous foramina of the vascular system (Fig. 3K–M). The wide base is curved, multipetaloid in shape, and with concave canal openings in the proximal view (Fig. 3M).

Morphotype 4

Four dermal denticles were found in the Kūmas quarry and three denticles in Karpėnai quarry. The 'tripod boomerang' shaped denticles which have three main lateral cusps, two of which are separated by two more grooves (Fig. 3N). The crown sits completely horizontally on the slender neck. The flat pedicle base is poorly preserved and has an indeterminate shape. These dermal denticles reach 0.2–0.3 mm in length.

Morphotype 5

Two hundred twenty-three euselachian dermal denticles were found in the Kūmas quarry and 84 denticles in Karpėnai quarry. The well-preserved drop-like crown margin surface is smooth, with some short ridges on the anterior side (Fig. 3O), which sits evidently obliquely up on the wide neck (Fig. 3P1). The crown length of the mesial platform (positioned in the centre of the upper crown's surface and running anterior to posterior) reaches 0.5 mm. The neck and crown's widths are almost the same, approximately 0.3–0.4 mm. The pedicle base is curved, multipetaloid in shape with concave canal openings in the proximal view. The subcrown is smooth, without any ornaments (Fig. 3P2). A less common crown surface is smooth, flat and 'anchor-like' in shape with a roundish posterior margin, while the anterior has six short convex ridges and two more evident lateral cusps. The crown sits horizontally on the massive neck, and reaches 0.4 mm in length and 0.25 mm in width. The pedicle base is curved and multipetaloid in shape (Fig. 3O).

Longitudinal and transverse sections of euselachian dermal denticles [VU-ICH-KAR-014, VU-ICH-KAR-016] reveal the presence of a thin layer of enameloid covering the top surface of the crown (Fig. 4A2–A5). This layer has a homogeneous thickness of around 0.005–0.0005 mm and gives the appearance of being composed of loose enameloid bundles oriented perpendicular to the crown surfaces. This can be better appreciated in the longitudinal section (Fig. 4B2–B3), whereas the poor preservation of the dermal denticles sectioned transversally only allows us to confirm the presence of the enameloid layer, but not its organisation.

The inner structure of an euselachian-type dermal denticle based on 3D-data is briefly described here [VU-ICH-KAR-023] (Fig. 5A). The complete vascular canal system can be divided into two major types based on their topological position in the studied fossil (Qu et al. 2015). The first type is placed on the neck and represented by five elongated, narrow and vertical canals, which are oriented almost perpendicular to the denticle base—a conventional pattern (Fig. 5A5–A6, A8–A9, A11–A12). It formed a 'bridge-like' structure—a second type, creating a junction between the more complicated and developed vascular system of the crown (Fig. 5A2–A3) and the base with a complex geometry. In general, the inner structure of euselachian dermal denticle has an interconnected system without any distinctly isolated details.

Morphotype 6

The rarest type (three microremains) were found in the Kūmas quarry and four denticles in Karpėnai quarry. The crown surface has been found in the studied quarry (Fig. 3Q1–Q2). The crown consists of two prominent ovoid parts, connected along their midline and mirroring each other, resting orthogonally on the base (Fig. 3Q1). The crown sits vertically on its base, reaching ~ 90° between these axes, thereby missing the neck, which is considered

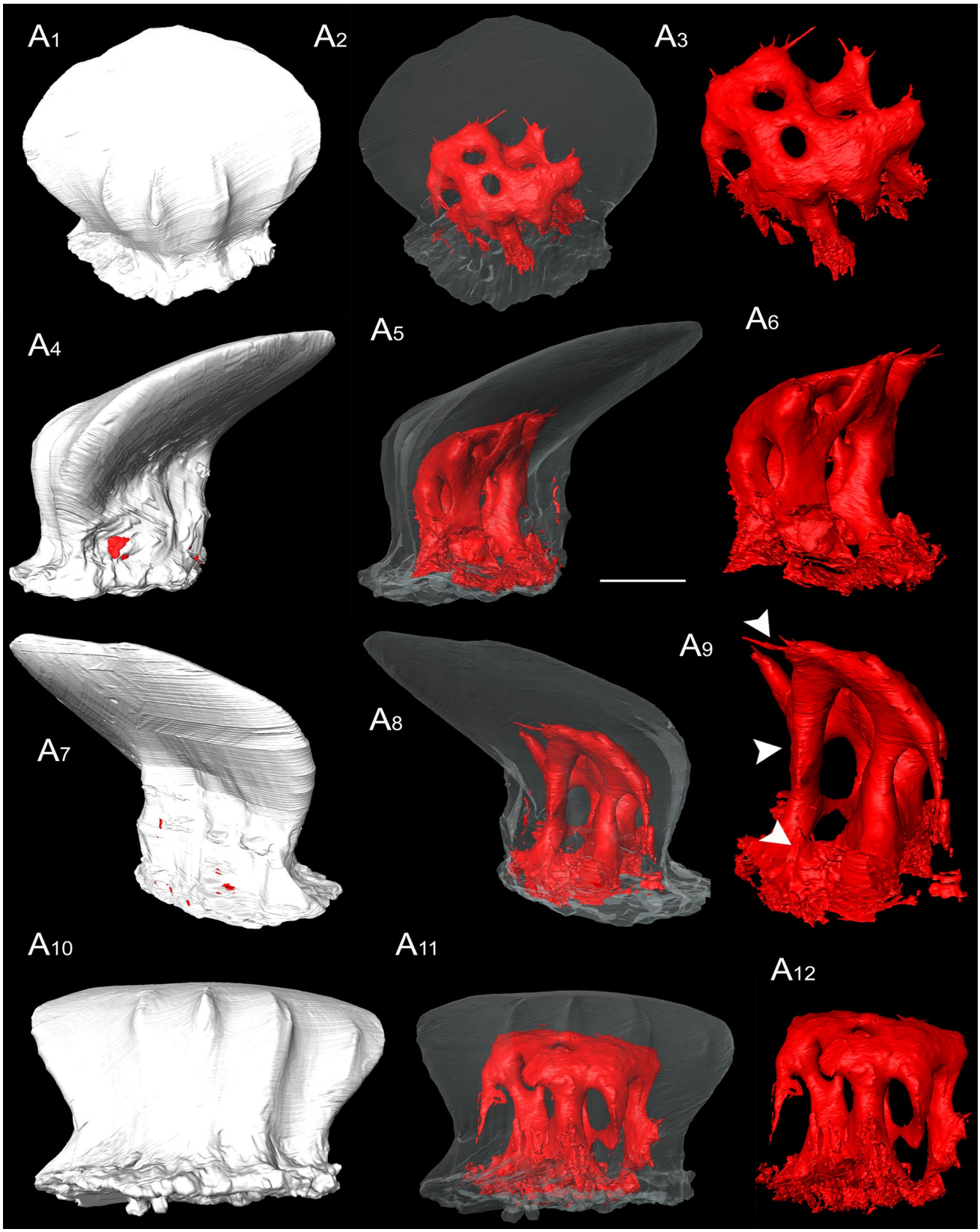
A1
A2
A3
A4
A5
A6
A7
A8
A9
A10
A11
A12

◂**Fig. 5** **A** 3D scanned euselachian-type dermal denticle [VU-ICH-KAR-023] from the KAR-4 sample, with details of the bone morphology and vascular system from the Karpėnai quarry. $\mathbf{A_1}$ External occlusal view; $\mathbf{A_2}$, $\mathbf{A_5}$, $\mathbf{A_8}$, $\mathbf{A_{11}}$ shade bone; $\mathbf{A_3}$, $\mathbf{A_6}$, $\mathbf{A_9}$, $\mathbf{A_{12}}$ vascular system with transparent bone contour; $\mathbf{A_4}$ lingual-lateral view; $\mathbf{A_7}$ oblique labial-lateral view; $\mathbf{A_{10}}$ occlusal view. Major types of inner structure indicated by the white arrows. The scale bar equals 0.1 mm

to be an important morphological feature of this type. The subcrown is smooth, without any ornaments (Fig. 3Q2). The pedicle base is roundish and ellipse-shaped with a very concave surface; no canal openings can be observed. The dermal denticle reaches 0.3 mm in width and 0.2 mm in length.

Superorder HOLOCEPHALI Bonaparte (1832)
Order HELODONTIFORMES Patterson (1965)
Family HELODONTIDAE Patterson (1965)
Genus *HELODUS* Agassiz (1838)
?HELODUS sp.
(Figs. 4C, 6)

Material

An isolated, well-preserved tooth from the Karpėnai quarry in northern Lithuania [VU-ICH-KAR-012] and a poorly preserved tooth from the Kūmas quarry in southern Latvia [VU-ICH-KUM-018].

Description

The poorly preserved isolated tooth from Kūmas quarry presented here as a small fragment, close to being bilaterally symmetrical and without any ornaments (Fig. 4C1–C2). It has an oval, partly broken coronal surface, which is convex, with smooth margins in posterior and one narrower sharp point in anterior face (Fig. 4C1). The roots are missing (Fig. 4C2). The tooth fragment reaches 0.8 mm in length and 0.5 mm in width. The well-preserved tooth from Karpėnai quarry is devoid of ornamentation; it is oval with smooth edge and one narrower sharp point (Fig. 4D2); has massive roots with numerous, randomly distributed foramina on the labial and lingual parts (Fig. 4D1).

The longitudinal section of the single ?*Helodus* sp. tooth reveals the presence of a well-differentiated cap of enameloid that coats its surface, with quite a distinct enameloid-dentine junction (EDJ) (Fig. 4D1–D3). This monolayer consists of a single crystallite enameloid (SCE) lacking any kind of organisation, with the enameloid crystallites randomly arranged (Fig. 4D5). The enameloid crystallites are round or subround (Fig. 4D5), and the EDJ is clear. Penetrating the enameloid layer, there are canals issuing from the dentine below (Fig. 4D3) nearly reaching the surface of the tooth (Fig. 4D4). The tubular dentine is occurred in the studied tooth (Fig. 4D3–4). The crown of the lateral tooth shows distinct features that reveal the internal tubular dentine. Part of this tissue (Fig. 3D3) runs parallel to one another and at almost right angles to the coronal surface of the tooth. Other part of the tissue is presented by the discontinues randomly distributed canals.

The 3D model of the ?*Helodus* sp. tooth (Fig. 6A1, A4, A7) shows a complete vascular system (Fig. 6A2–A3, A5–A6, A8) which consists of some major types of pore cavities (see the white arrows in Fig. 6A9). Most of the cavities are single and isolated from the other cavities. Another type is paired, with a small shared basal part close to the junction between the pore cavities and canal. A third type shares a larger basal portion with the two cavities diverging in a higher position. The last type is in an extreme condition, with the two pore cavities diverging at a position close to the surface of the tooth (Qu et al. 2015). The vertical, narrow and elongated pore cavities are oriented obliquely and perpendicular to the tooth base.

Remarks

The tooth has the same morphological features as a well-preserved ?*Helodus* tooth [VU-ICH-KAR-012] from the Naujoji Akmenė Formation of the late Permian in northern Lithuania (Dankina et al. 2017). Also, the general shape of this tooth is comparable to a *Helodus* tooth from the Permian in western Australia (Teichert 1943). As well, Permian *Helodus* are known from Ural Mountains (Obruchev and Orlov 1964) and Texas, USA (Johnson 1981). Moreover, the base consists of an osteodentine tissue according to Glikman (1964) who has proposed elasmobranch teeth microscopic anatomical character. This histological organisation is similar to one that was found in the tooth plate of a Carboniferous *Helodus* from England, although the enameloid layer in our tooth is thicker (Gillis and Donoghue 2007). The trabecular dentine and parallel vascular canals are one of the main characteristics of this taxon (Stahl 1999).

Superclass OSTEICHTHYES Huxley (1880)
Class ACTINOPTERYGII Cope (1887)
(Figs. 7, 8, 9)

Scales

Two hundred twelve scales with a well-preserved ganoine outer layer were found in the Kūmas quarry in southern Latvia and nine scales in Karpėnai quarry in northern Lithuania. All these scales were classified into six morphotypes based on their morphological features, which are shown in the 14 selected samples [VU-ICH-KUM-019–VU-ICH-KUM-032]. The scales were identified based on their morphological features according to their specific fish body sectors as anterior-mid lateral flank, posterior lateral flank, ventral flank, pectoral peduncle, and unknown location scales (Hamel 2005;

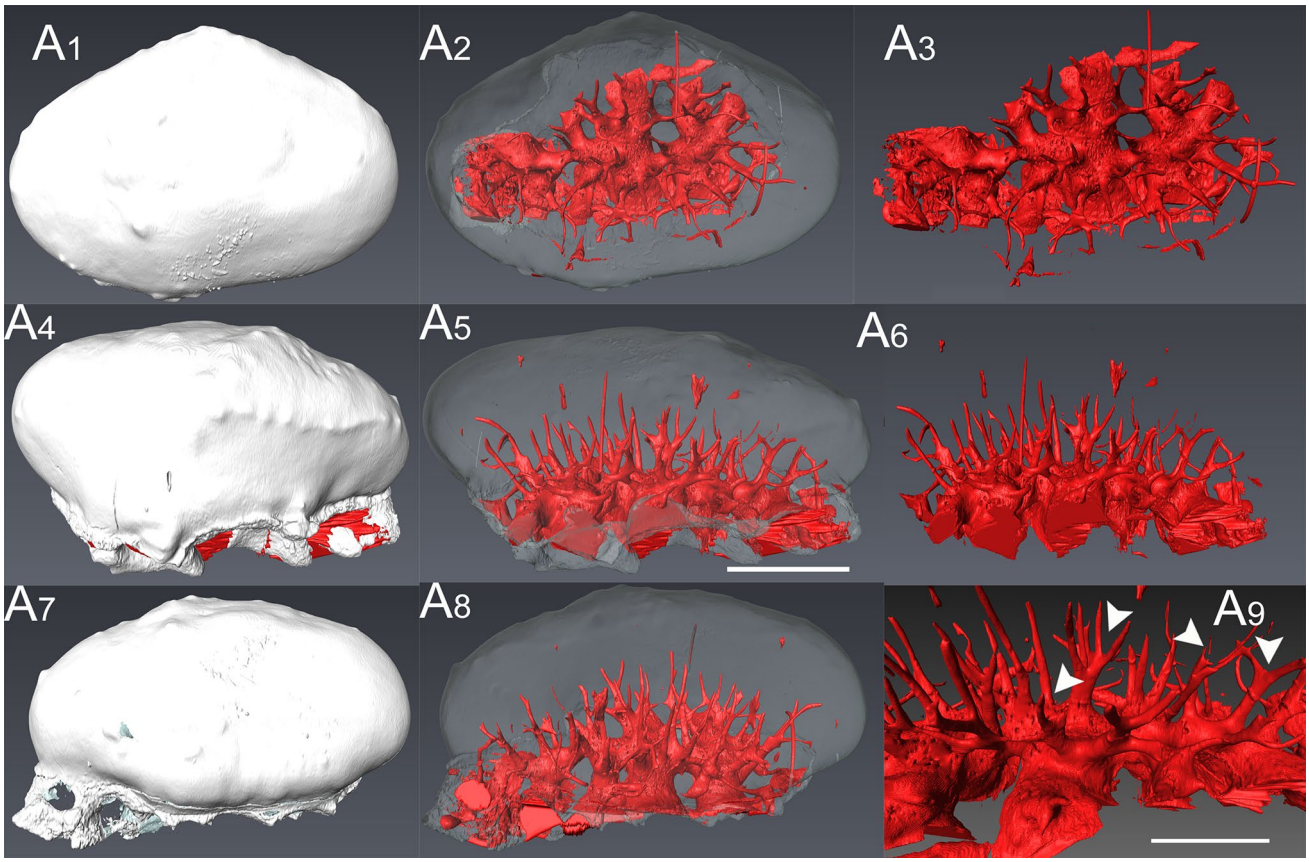

Fig. 6. 3D model of the scanned ?*Helodus* sp. tooth [VU-ICH-KAR-012] from the KAR-7 sample showing more details of the entire canal system from the Karpėnai quarry. $\mathbf{A_1}$ External view; $\mathbf{A_2}$, $\mathbf{A_5}$, $\mathbf{A_8}$ shade bone; $\mathbf{A_3}$, $\mathbf{A_6}$, $\mathbf{A_9}$ vascular system with transparent bone contour; $\mathbf{A_4}$ lingual-lateral view; $\mathbf{A_7}$ oblique labial-lateral view. Major types of pore cavities indicated by white arrows. The scale bars are equal to: 1.0 mm $\mathbf{A_1}$, $\mathbf{A_2}$, $\mathbf{A_3}$, $\mathbf{A_4}$, $\mathbf{A_5}$, $\mathbf{A_6}$, $\mathbf{A_7}$, $\mathbf{A_8}$ and 0.25 mm $\mathbf{A_9}$

Štamberg 2010; Chen et al. 2012). As a result, the described scales can be divided into six morphotypes.

Morphotype 1

One hundred and eighty-sixth scales were found in the Kūmas quarry and eight scales in Karpėnai quarry. These scales related to the posterior lateral flank and caudal peduncle body sectors (Fig. 7A–D). They are rhombic or diamond shaped, sometimes gently convex in their central part (Fig. 7A, C), but more commonly with a flat surface (Fig. 7B, D). An examination of these scales with SEM disclosed numerous small, roundish-shaped microtubercles in the outer ganoine layer (Fig. 7B). The surface is smooth, but some scales have fine, short groove ornaments whose direction may go from the anterior to the posterior margins of a scale (Fig. 7B). Only one of the specimens shows a delicate perpendicular striation. The scales have some notable canal openings on top of the surface (white arrow in Fig. 7A). The scale margins formed two obtuse (dorsal, ventral) and two acute (anterior, posterior) angles.

Morphotype 2

Four specimens of this morphotype were found (Fig. 7E–F) in Kūmas quarry. These are the anterior-mid lateral flank scales. Elongated rhombic-shaped scale with almost right (~ 90°) or right-angles at all four corners, while the other lacks it. The base is thick and convex (Fig. 7E) or slightly narrow and flat (Fig. 7F). One scale has a peg articulation (Fig. 7E) while other doesn't (Fig. 7F). The ganoine-covered field is ornamented by several transverse inter-ridge grooves over the middle part of the surface. The scale is 1.8 mm in dorsoventral and 0.7 mm in anteroposterior direction.

Morphotype 3

Four scales of this type are located on the ventral flank sector (Fig. 7G–H). They are generally elongated (Fig. 7G); some scales are square shaped (Fig. 7H), thick, with a slightly twisted posterior corner and other obtuse or almost right-angles. The ganoine outer tissue has a microtubercle pattern and covers about 0.75 mm of the scale field. The surface

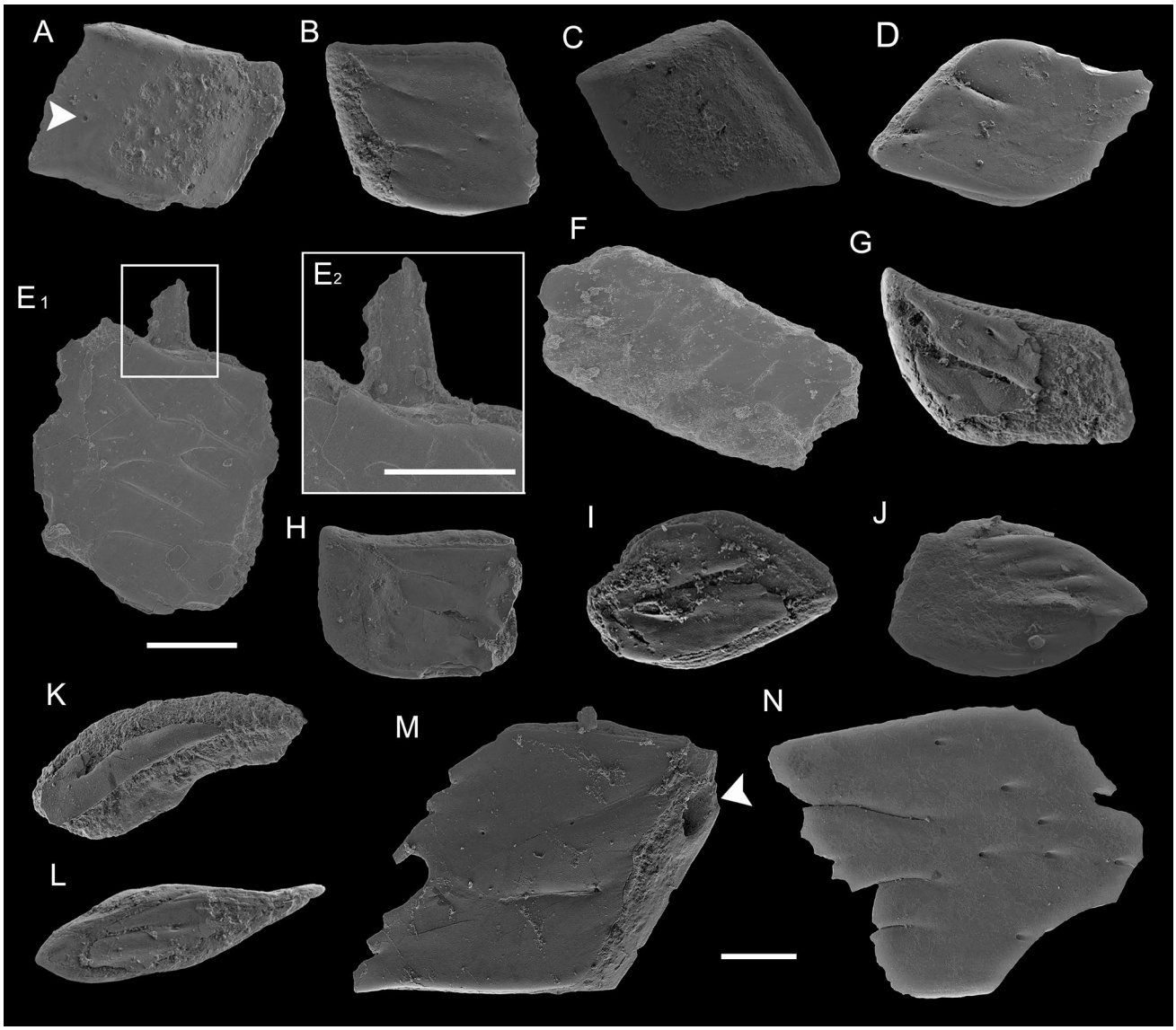

Fig. 7 SEM images of isolated actinopterygian scales from the Kūmas quarry. **A–D** Morphotype 1. **A** VU-ICH-KUM-019, from the KUM-2 sample; **B** VU-ICH-KUM-020, from the KUM-2 sample; **C** VU-ICH-KUM-021, from the KUM-2 sample; **D** VU-ICH-KUM-022, from the KUM-2 sample. **E–F** Morphotype 2. **E** VU-ICH-KUM-023, from the KUM-10 sample; $\mathbf{E_1}$ a general view; $\mathbf{E_2}$ a detailed peg view in external view. **F** VU-ICH-KUM-024, from the KUM-3 sample. **G–H** Morphotype 3. **G** VU-ICH-KUM-025, from the KUM-2 sample; **H** VU-ICH-KUM-026, from the KUM-2 sample. **I–J** Morphotype 4. **I** VU-ICH-KUM-027, from the KUM-2 sample; **J** VU-ICH-KUM-028, from the KUM-2 sample. **K–L** Morphotype 5. **K** VU-ICH-KUM-029, from the KUM-2 sample; **L** VU-ICH-KUM-030, from the KUM-2 sample. **M–N** Morphotype 6. **M** VU-ICH-KUM-031, from the KUM-2 sample; **N** VU-ICH-KUM-032, from the KUM-7 sample. All of the material is pictured in apical view. The white arrows show a canal opening on top of the surface (**A**) and the anterior entry of the lateral line canal (**M**). The scale bars are equal to: 0.1 mm (**A–D**, $\mathbf{E_1}$, **F–N**), 0.05 mm ($\mathbf{E_2}$)

has some canal openings and a short, narrow concave ridge ornament whose direction may go from the anterior to the posterior margins of a scale. Their anteroposterior reaches 1.0 mm and dorsoventral is 0.4–0.6 mm.

Morphotype 4

Ten scales were found in the Kūmas quarry and one scale in Karpėnai quarry. These scales belong to the pectoral peduncle sector (Fig. 7I–J). They are small, elongated and ellipsoid shaped, with an acute angle of the posterior corner and a slightly obtuse anterior corner. Their posterior and dorsal margins are considerably longer than their anterior and ventral margins. Three quarters of the surface are covered by ganoine tissue, with a roundish microtubercle pattern (Fig. 7I); some scales have overlapping wide convex ridges (Fig. 7J), growing in the anterior–posterior direction. There is no peg-and- socket on the thick base. These scales

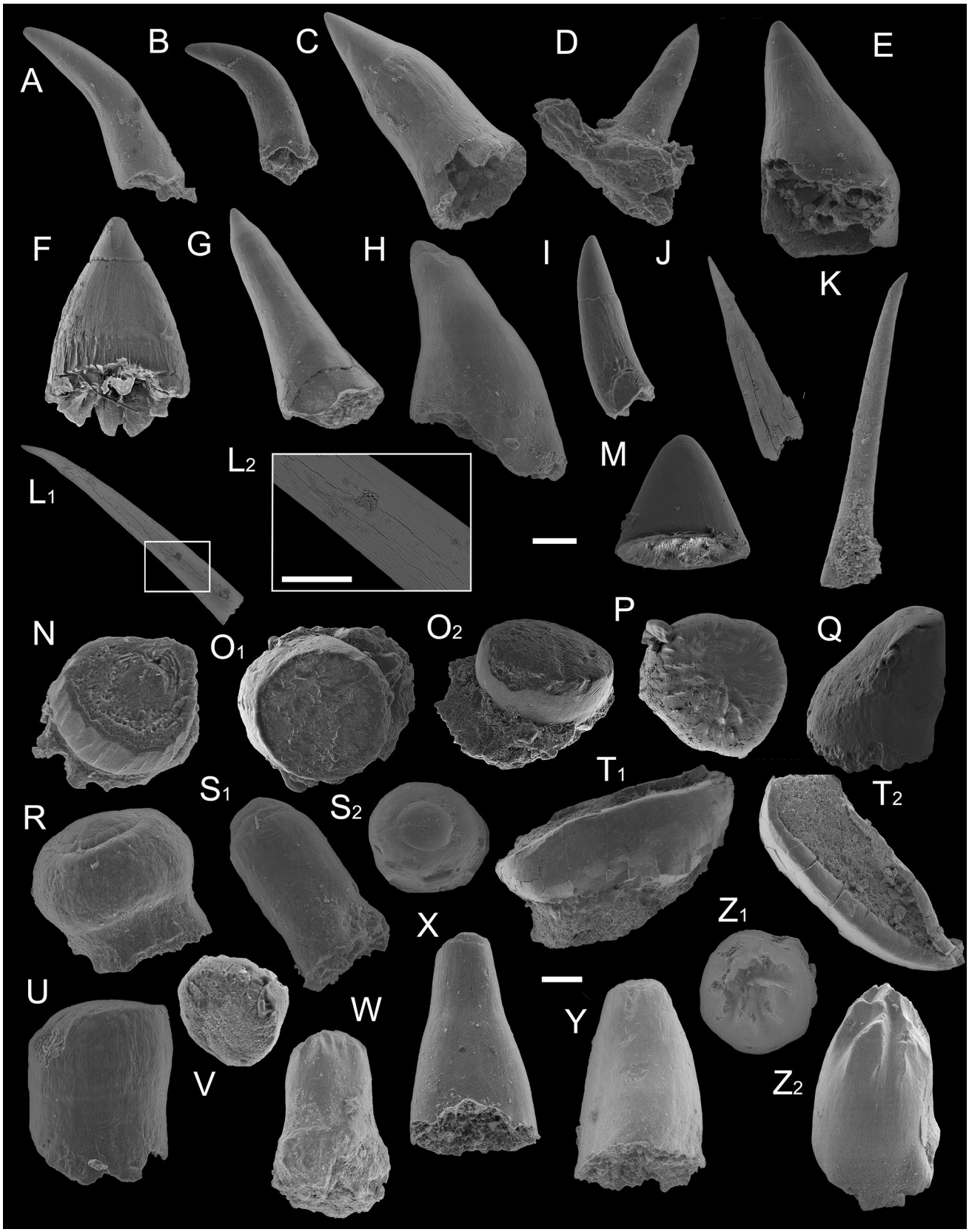
A
B
C
D
E
F
G
H
I
J
K
L1
L2
M
N
O1
O2
P
Q
R
S1
S2
T1
T2
U
V
W
X
Y
Z1
Z2

◂**Fig. 8** SEM images of the different shaped actinopterygian teeth assemblage from the Kūmas quarry. **A**–**M** Morphotype 1. **A** VU-ICH-KUM-033, from the KUM-4 sample. **B** VU-ICH-KUM-034, from the KUM-3 sample. **C** VU-ICH-KUM-035, from the KUM-3 sample. **D** VU-ICH-KUM-036, with a preserved fragment of the base from the KUM-3 sample. **E** VU-ICH-KUM-037, from the KUM-4 sample. **F** VU-ICH-KUM-038, from the KUM-1 sample. **G** VU-ICH-KUM-039, from the KUM-4 sample. **H** VU-ICH-KUM-040, from the KUM-3 sample. **I** VU-ICH-KUM-041, from the KUM-10 sample. **J** VU-ICH-KUM-042, from the KUM-2 sample. **K** VU-ICH-KUM-043, from the KUM-3 sample. **L** VU-ICH-KUM-044, from the KUM-4 sample; $\mathbf{L_1}$ general view; $\mathbf{L_2}$ microtubercles structure of tooth. **M** VU-ICH-KUM-045, from the KUM-9 sample in lateral view. **N**, **O** Morphotype 2. **N** VU-ICH-KUM-046 in oblique occlusal view from the KUM-9 sample. **O** VU-ICH-KUM-047, from the KUM-3 sample; $\mathbf{O_1}$ in occlusal view; $\mathbf{O_2}$ in lateral view. **P**, **Q** Morphotype 3. **P** VU-ICH-KUM-048 in occlusal view from the KUM-5 sample. **Q** VU-ICH-KUM-049 in lateral view from the KUM-3 sample. **R**–**T** Morphotype 4. **R** VU-ICH-KUM-050 in lateral view, from the KUM-3 sample. **S** VU-ICH-KUM-051, from the KUM-4 sample, $\mathbf{S_1}$ in lateral view; $\mathbf{S_2}$ in occlusal view. **T** VU-ICH-KUM-052, from the KUM-5 sample, $\mathbf{T_1}$ in lateral view; $\mathbf{T_2}$ in occlusal view. **U**, **V** Morphotype 5. **U** VU-ICH-KUM-053 in lateral view from the KUM-4 sample. **V** VU-ICH-KUM-054 in oblique occlusal view from the KUM-4 sample. **W**–**Z** Morphotype 6. **W** VU-ICH-KUM-055 in lateral view from the KUM-4 sample. **X** VU-ICH-KUM-056 in lateral view from the KUM-4 sample. **Y** VU-ICH-KUM-057 in oblique lateral view from the KUM-4 sample. **Z** VU-ICH-KUM-058, from the KUM-3 sample; $\mathbf{Z_1}$ in oblique lateral view; $\mathbf{Z_2}$ in occlusal view. The scale bars are equal to: 0.1 mm (**A**–$\mathbf{L_1}$, **M**–**S**, **U**–**Z**), 0.05 mm ($\mathbf{L_2}$) and 0.3 m (**T**)

reach 0.6–0.8 mm in anteroposterior and 0.4–0.5 mm in dorsoventral direction.

Morphotype 5

Four scales were found in the Kūmas quarry. This type is represented by fulcral scales which are not well-preserved (Fig. 7K–L). They are generally small, thick and rod-like, or, more precisely, with an extremely elongated shape and a flat, slightly massive surface, three-quarters covered by ganoine tissue. The ganoine-covered field is sculpted by tiny, roundish microtubercles and has no ornaments. These scales' antero-dorsal corners are tapering; their margins look convex, while their postero-ventral corners are acute, lightly concave, very narrow and a ganoine layer is absent along postero-ventral corner. These scales are 1.0 mm in anteroposterior and only 0.2–0.3 mm in dorsoventral direction.

Morphotype 6

Four scales were found in the Kūmas quarry. This type of scale belongs to an undetermined fish body sector, because the material is not completely preserved (Fig. 7M–N). These samples comprise straight dorsal, ventral and anterior margins, while their entire posterior margins are pectinated, with several narrow serrations. The ganoine-covered field has a tiny, roundish microtubercle pattern. Some scales are smooth, showing flask-shaped pore cavities that are visible through the translucent ganoine layer (Fig. 7N). Sometimes, the anterior margin is thick and massive with a significantly wide anterior entry of the lateral line canal (see the white arrow in Fig. 7M); pegs and anterodorsal process are missing. The scales are 1.3–1.5 mm in anteroposterior and 1.0 mm in dorsoventral direction.

Teeth

One thousand six hundred ninety-three well-preserved isolated teeth have been found in the Kūmas quarry in southern Latvia and 98 teeth in the Karpėnai quarry in northern Lithuania. The teeth are represented by the 26 various pictured microremains [VU-ICH-KUM-033–VU-ICH-KUM-058] and divided into six morphotypes based on their different morphological characteristics.

Morphotype 1

One thousand six hundred and sixty-seventh teeth were found in the Kūmas quarry and 94 teeth in Karpėnai quarry. Varied assemblage of conical, thin, light amber-coloured teeth (Fig. 8A–M). Most of the teeth are slender, smooth, with no distinct visible sculpture, although the microtubercles are well developed (Fig. 8C, E, J, L). They cover the whole surface of the tooth, with the exception of the acrodin cap. The microtubercles are proximo-distally elongated, narrow and blend together in oblique rows (Fig. 8L2). These teeth are 0.3–4.0 mm in length and 0.09–0.3 mm in width. Most teeth are straight with wider dentin cones and bases (Fig. 8C, E, F, H). These teeth do not have any distinct sculpture and could reach a maximum width or length measurement of 0.6 mm. Rare teeth are elongated, smooth, with a curved 'horn-like' shape with slightly blunt transparent acrodin cap (Fig. 8A–B). These teeth reach 0.3–0.6 mm in length and 0.05–0.2 mm in width. Very rare teeth are represented only by the acrodin cap (Fig. 8M).

A SEM histological analysis of the teeth belonging to morphotype 1 (Fig. 9A1, B1) reveals an enameloid layer, dentine core and central pulp cavity (Fig. 9A2). The enameloid extends only over the apical part of the tooth, attaining its maximum thickness at the base of the cap, where it reaches 70 µm (Fig. 9A3). Lingually and labially, the enameloid layer is reduced to 5 µm (Fig. 9A4–A5). The hypermineralised layer is composed of single crystallites with different organisations (Štamberg 2016), depending on in which part of the layer they are embedded. Lingually and labially, the layer is composed of individual crystallites parallel to each other and oriented perpendicular to the tooth surface, without any kind of higher form of organisation (Fig. 9A5). At the base of the cap, where the layer is thicker,

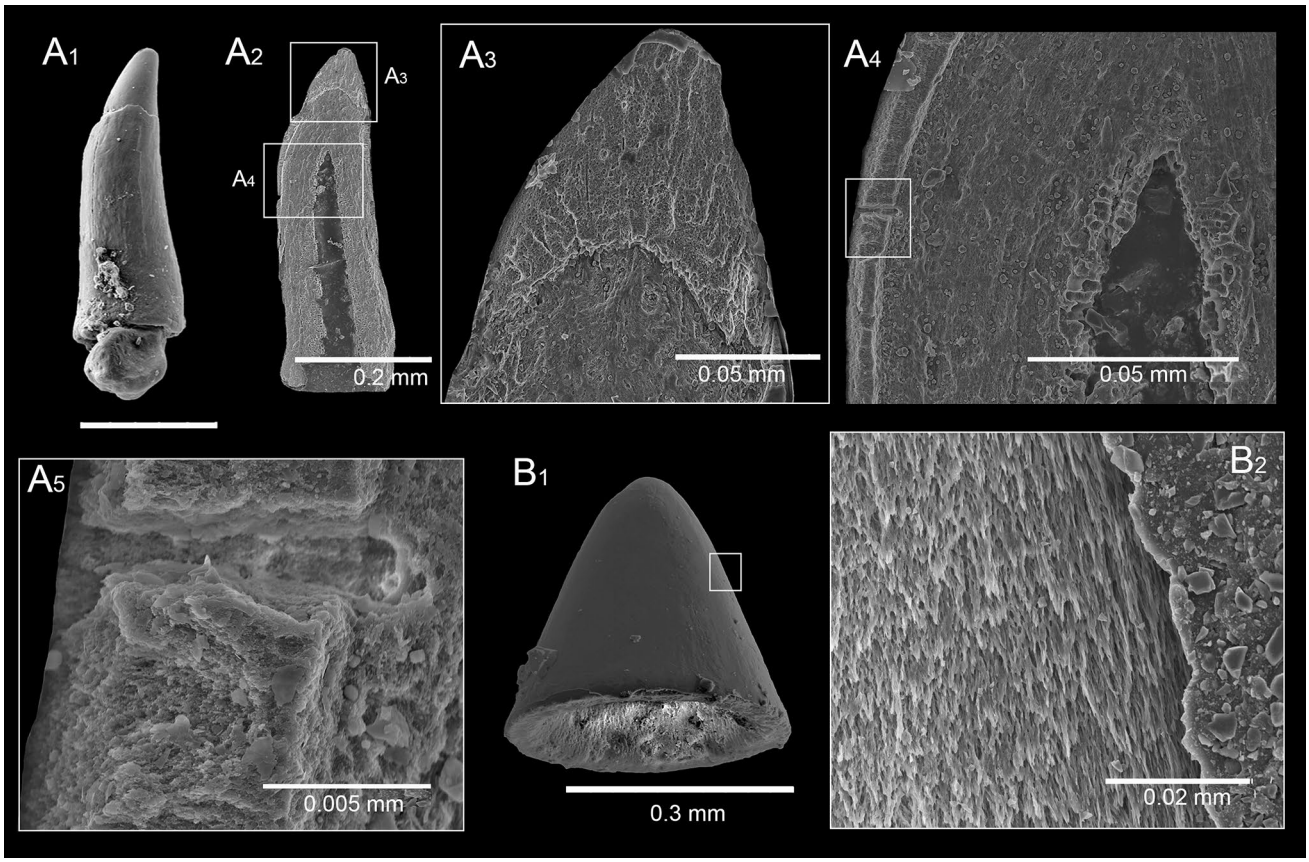

Fig. 9 Histology of actinopterygian teeth from the Kūmas quarry. $\mathbf{A_1}$ General view of the tooth [VU-ICH-KUM-059] from the KUM-2 sample; $\mathbf{A_2}$ the entire longitudinal sectioned tooth showing the enameloid layer, dentine core and central pulp cavity; $\mathbf{A_3}$ an enameloid layer in detail; $\mathbf{A_4}$ a collar enamel; $\mathbf{A_5}$ individual crystallites parallel to each other and oriented perpendicular to the tooth surface. $\mathbf{B_1}$ General view of the acrodine cap [VU-ICH-KUM-045] from the KUM-9 sample; $\mathbf{B_2}$ enameloid cap showing any crystallites' orientation

the enameloid crystallites are organised in loose bundles (Fig. 9A3) that display a tendency to be oriented parallel to the tooth surface (Fig. 9B2). The teeth do not show any kind of superficial layer, which may have been worn down. The enameloid-dentine junction (EDJ) is clearly distinguishable and regular.

Morphotype 2

Two teeth were found in Kūmas quarry. Teeth have a rod-shaped, short, cylindrical shape with a flat apex (note: the tooth cap was probably lost?) (Fig. 8N–O_1). Some teeth have multiple vertical, convex ridges which can cover an entire lateral margin and with a visible, enameloid, dentine tissue inner structure in the cross section in the apical view (Fig. 8N). The other teeth only have well-developed, vertically elongated, narrow microtubercles in the lateral view with a smooth rubbed apex (Fig. 8O2). These teeth reach a maximum of 0.5 mm in diameter and 0.2 mm in height.

Morphotype 3

Eight teeth were found in the Kūmas quarry and two teeth in Karpėnai quarry. This morphotype has the eight isolated teeth. Seven of the teeth are semispherical, convex and with a circular surface shaped in the apical view. The entire crown exhibits irregular and radiating ridges which do not join in the central part of the cap (Fig. 8P). The microtubercles are well developed and are proximo-distally elongated, narrow, and blend together in oblique rows. These teeth are a maximum of 1.2 mm in diameter and 0.5 mm in height. A single pycnodont-like tooth has an asymmetrical conical crown with a straight, slightly convex labial-lateral margin and a relatively narrow occlusal platform that is confluent with the strongly concave lingual face (Fig. 8Q). This tooth reaches 1.0 mm in height and 0.7 mm in base width.

Morphotype 4

Seven teeth were found in the Kūmas quarry and one tooth in Karpėnai quarry. This morphotype includes six

crushing-type teeth (Fig. 8R–S) and one isolated dental remain (Fig. 8T). The crushing teeth represented here are globular (Fig. 8R) and circular-rod (Fig. 8S) shaped in the lateral view, and with convex, tiny, sometimes wide, hemispherical acrodine caps in the apical view. The crown is smooth, with no distinct visible ornaments. Only the roots are missing. These teeth can reach 0.1–0.5 mm in diameter and 0.4–0.6 mm in height. While the massive dental remain has a long axis parallel to the labial margin, it has a narrow and bilaterally symmetrical shape with a slightly depressed oval, thick, and ring-like rim in the enameloid layer in the apical view (Fig. $8T_1$). The tooth crown is smooth, its central indent is shallow and filled with outer sediments (Fig. $8T_2$). The base is broad and partly preserved. It is 2.5 mm in length, 0.6 mm in width and 1.1 mm in height.

Morphotype 5

Five isolated teeth (Fig. 8U–V) were found in the Kūmas quarry. The crushing dentitions are spherical or styliform shaped in the lateral view (Fig. 8U) with a circular surface and flat, smooth crown tip in the apical view. No visible ornaments were obtained (Fig. 8V). These teeth reach 0.4–0.5 mm in height and 0.25 mm in diameter.

Morphotype 6

Four teeth were found in the Kūmas quarry and one tooth in Karpėnai quarry.Several teeth which are conical in shape and covered with microtubercles which are proximo-distally elongated, narrow and blend together in oblique rows. The crown has features comprising irregular and radiating ridges which create a blunt (Fig. 8 W) or slightly acute (Fig. 8Z) central part of the cap. Sometimes, the tooth caps are devoid of any ornamentation (Fig. 8X–Y). These teeth reach 0.5 mm in height and 0.3 mm in diameter.

5 Discussion

The fish assemblage of the Naujoji Akmenė Formation is hard to identify taxonomically because of the lack of comparative material. However, it includes the shallow-water fish fauna based on isolated remains such as actinopterygian and chondrichthyans. The fish remains occur in the carbonate sediments that deposited during the first transgressive cycle of Zechstein Sea. This transgression was the biggest and reached the most north-eastern part of Zechstein sea as a present-day the territory of Lithuania and Latvia.

Late Palaeozoic actinopterygian is widely distributed taxon in the Zechstein Sea. The complete and almost complete fish trunks were common in the Permian of the Germany (Diedrich 2009), England (King 1850), eastern Greenland (Aldinger 1937; Nielsen 1952) and Poland. In Germany and England, actinopterygian fossils were determined as *Pygopterus humboldti*, *Acrolepis sedgwickii*, *Acrolepis digitate*, *Palaeoniscus* sp., *P. freieslebeni, P. longissimus, P. macropthalmus, Acrolepis* sp., *Platysomus* sp., *P. gibbosus*, *Globulodus* sp., *Dorypterus* sp. (King 1850; Woodward 1891); *Elonichthys* sp., *Globulodus* sp., *Platysomus* sp. have been mentioned from Upper Permian of Greenland (Aldinger 1937); *Palaeoniscus vratislaviensis* was found in the Permian of Poland (the specimen is stored in the American Museum of Natural History in NYC, United States). Moreover, many isolated actinopterygian remains were earlier found and determined as *Elonichthys* sp., *Platysomus* sp., Haplolepidae indet., Pycnodontidae indet., Palaeonisciformes indet. in the Upper Permian of the Lithuania (Dankina et al. 2017). The morphotype 3 of actinopterygian teeth have similar circular tooth with radiating margin ridges has been illustrated and identified as cf. *Anomoeodus* from the Sao Khua Formation of the Cretaceous at Phu Phan Thong in Thailand (Cavin et al. 2009). Moreover, the studied tooth has shape similarities of Pycnodontiformes indet. from the Lower Cretaceous in Tunisia (Cuny et al. 2010). Identical-shaped teeth were found previously in the Naujoji Akmenė Formation of the Upper Permian in Lithuania (Dankina et al. 2017). A similar robust conical-crowned tooth shape was found in the Upper Cretaceous in Bulgaria (Andreev 2011). The morphotype 4 of actinopterygian teeth include a similar vomerine tooth plate of *Macropycnodon streckeri* was found in the Juana Lopez Member of the Upper Cretaceous in New Mexico (Shimada et al. 2010) and cf. *Coelodus* sp. vomers from the Csehbánya Formation of the Upper Cretaceous in Hungary (Szabó et al. 2016). Moreover, morphologically similar crushing-type teeth were identified as aff. *?Gyrodus* sp. from the Lower Cretaceous in the Baltic Sea (Kriwet and Schmitz 2005). However, another similar globular and conical tooth with a small central 'wart' was assigned to *Lepidotes* sp. from the Middle Jurassic of the Grands Causses in southern France (Knoll et al. 2013). Despite all the shape similarities which are mentioned above, the studied material from this group needs more detailed taxonomic analyses and well-preserved samples, allowing a microstructural and histological investigation. The morphotype 5 of actinopterygian teeth have the morphologically similar to the Lepisosteiformes order based on some fish findings, their images and descriptions from the Wessex Formation of the Lower Cretaceous on the Isle of Wight in southern England (Sweetman et al. 2014).

Permian euselachian is commonly spread in the eastern, central and western part of the Zechstein Sea. This taxon is known from the Permian of the Lithuania (Dankina et al. 2017); Greenland (Nielsen 1932; Bendix-Almgreen 1975); *Hopleacanthus richelsdorfensis* occurs in the Germany (Schaumberg 1982; Diedrich 2009). The morphotype 3

similar roundish scale was interpreted as being a ?hybodont/synechodontiform scale from the Lower Triassic in Oman (Koot et al. 2015). An elongated semi-roundish scale (similar to the ones described in this work) was also found and assigned to Hybodontidae gen. et sp. indet. from the Triassic in Spitzbergen (Reif 1978). The morphotype 4 similar "tripod" shape of the crown was assigned to Hybodontidae denticles from late Triassic in the central Germany (Reig 1978). The morphotype 5 similar dermal denticle crown surface with these features was identified as a hybodontiform scale from the Middle Triassic in Spain (Manzanares et al. 2014). The similar histological organisation of this morphotype has also been described in the dermal denticles of some Mesozoic Hybodontiformes and living neoselachians (Manzanares et al. 2014); however, in the dermal denticles of the neoselachians, there appear to be two 'sublayers'; the outer sublayer is composed of compacted crystals and the inner sublayer has crystals showing a preferred orientation that is perpendicular to the crown's surface (Manzanares et al. 2014). The morphotype 6 similar wide opening for the pulp cavity scales can be observed in Devonian thelodonts (Örvig 1969).

The *Acrodus* sp. and *Helodus* sp. are rare finds in the Permian of Zechstein Sea. Only few *Helodus* sp. fossils are known from the Permian of the Greenland (Bendix-Almgreen 1975) and Upper Permian of the Lithuania (Dankina et al. 2017). *Helodus* sp. finds in the Lithuania and Latvia could possibly extent this taxon into Upper Permian. *Acrodus* sp. spread during Permian of the other palaeogeographical aquatic environments which are current represent territory of the modern Texas (Johnson 1981), Japan (Goto et al. 1988) and Iran (Hampe et al. 2013) and has been never found in the Zechstein Sea before. However, Hybodontiformes indet. was reported from Permian of Greenland (Nielsen 1932).

Omanoselache sp. is not common in the late Palaeozoic chondrichthyan assemblage. *Omanoselache hendersoni* and *O. angiolinii* occur in the Khuff Formation (Wordian) of the central eastern Oman (Koot et al. 2013) but this taxon is more spread out in the Triassic of Oman (Koot et al. 2015), China (Chen et al. 2007) and Spain (Manzanares et al. 2018). These species have been never found in the Upper Permian of Zechstein Sea before.

A similar late Permian assemblage of isolated chondrichthyan and osteichthyan fossils was found previously and described on the eastern side of Zechstein Basin based on the Karpėnai quarry in northern Lithuania (Dankina et al. 2017). A comparison of fish fossil abundances from roughly similar total samples (~210 kg in weight) of limestone between the Karpėnai and Kūmas quarries revealed a significant difference (Fig. 2). The total actinopterygian teeth number is ~120 times and actinopterygian scales number is ~23 times more abundant in the Latvian quarry than in Lithuanian quarry. The difference in the influx of fresh water from the surrounding terrain towards the hypersaline Zechstein Basin was possibly a major factor that affected the differences in abundance of the fossil material between the Kūmas locality (southern Latvia), which was much closer to the shoreline (and thus a riverine source of water), and the Karpėnai locality (northern Lithuania), which was farther offshore (Magaritz 1987; Peryt and Scholle 1996). The Zechstein Basin was a significantly restricted sea with sedimentation that resembled giant playa-like sequences, where hypersaline waters in the central part gave rise to evaporites together with carbonates, while more fresh water environments near the shoreline were suitable for the development (precipitation) of limestones (Kendall 1984). Therefore, the current observations of the abundance and diversity gradient are in accordance with the explanation that at the major factor that determined the greater richness of fossil ichthyofauna in the Kūmas locality compared to the southern Karpėnai locality is the salinity gradient. The distribution of anhydrites and gypsum, which are abundant in the correlates of the Naujoji Akmenė Formation in central Lithuania and Kaliningrad Oblast in Russia (Paškevičius 1997), suggest that the salinity gradient increased in a south-westerly direction from the studied sites, thus probably physiologically restricting the possible distribution of fish faunas. In addition to the salinity stress, ichthyofaunas which existed in the offshore parts of the Zechstein sea should have experienced stronger cytotoxic effects of halogenated hydrocarbons. Halophilic bacteria, a major source of volatile halogenated hydrocarbons, thrive in modern hypersaline basins such as Kara Bogaz Gol, which are thought to be closely environmentally analogous to the hypersaline parts of the Zechstein Sea (Weissflog et al. 2009). Also, the variation in abundance of fish microremains in Naujoji Akmenė Formation could be explained by regional variations in fresh water input during episodic exposure events associated with regional or global sea-level fluctuations (Peryt and Scholle 1996). In addition to the listed factors, the restricted hypersaline offshore conditions, with the abundance of dissolved sulfates, promote anaerobic and possibly euxinic conditions, which should have adversely affected ichthyofaunas. Fluctuations in anoxi/euxinic zones in modern restricted basins on a regular basis cause significant fish die-offs (Meyer and Kump 2008). This suggestion is supported by the abundant bituminous material which was released after dissolution of limestones and dolostones of the offshore settings representing Karpėnai locality in Lithuania (Dankina et al. 2017). The differences in abundance of ichthyolites (denticles, and scales) between two locations are highly contrasting through whole studied geological sections, which shows systemic nature of observed feature (Tables 1, 2).

Table 2 Abundance of palaeoichthyofaunal microremains from the Karpėnai quarry

Sample	Height, m	Chondrichthyan							Actinopterygian											
		Tooth	Scale						Tooth						Scale					
			M1	M2	M3	M4	M5	M6	M1	M2	M3	M4	M5	M6	M1	M2	M3	M4	M5	M6
KAR-13	13.0–14.0				1		1		1											
KAR-12	12.0–13.0						2		4											
KAR-11	11.0–12.0						6		2											
KAR-10	10.0–11.0						10		5											
KAR-9	9.0–10.0			10	1		10		8		1	1			2					
KAR-8	8.0–9.0				1	1	17	2	8											
KAR-7	7.0–8.0	1				1	1				1									
KAR-6	6.0–7.0						3		1											
KAR-5	5.0–6.0						9		16											
KAR-4	4.0–5.0			1		1	12		14						1					
KAR-3	3.0–4.0				2		4		19						4					
KAR-2	2.0–3.0			4			5	2	9					1	1					
KAR-1	0.0–2.0				2		4		7									1		
Total	14.0	1		15	7	3	84	4	94		2	1		1	8			1		

6 Conclusion

The new chondrichthyan and osteichthyan material from late Permian of Kūmas quarry (southern Latvia) presented here adds new data to the scarce ichthyofaunal fossil record of the north-eastern Zechstein Basin margin.

1. An influx of fresh water could have caused the differences in fossil abundance between the more offshore Karpėnai locality and the nearshore Kūmas locality of the Zechstein Basin. The well-bedded limestone of the Naujoji Akmenė Formation is easily correlatable with the Sātiņi, Kūmas, and Alši Formation limestones.
2. The numerous isolated fish microremains belong to indeterminate Actinopterygii and the following groups of Chondrichthyes represented by various dermal denticles and teeth from Euselachii, ?*Acrodus* sp., ?*Omanoselache* sp., and holocephalan helodontiform.
3. SEM imaging analysis revealed that late Permian fish (chondrichthyans, actinopterygians) teeth possessed an outer homogeneous layer of SCE described by a matrix of randomly orientated (fluor-) hydroxyapatite crystallites with a non-preferred orientation.
4. 3D-models of the vascular system and dentine of an euselachian-type dermal denticle and a ?*Helodus* sp. tooth from the late Permian are visualised here. The synchrotron segmentation technique demonstrated and provided important information about the analysed fossils' microanatomical structure and virtual histology without damaging the fish microremains. This 3D-data will thus be essential for fully understanding the fish fossils' architectural internal canal diversity and external morphological features for comparative studies in the future.

Acknowledgements The authors would like to thank J.-P. M. Hodnett, J. Fischer, I. Kogan, R. Figueroa, A. Chahud and anonymous reviewer for significantly improving the manuscript. Also, I. Celiņš (CEMEX company, Latvia), who accompanied us to the Kūmas quarry, and D. Šiupšinskas (Vilnius University, Lithuania), who helped to collect and safely transport the samples. We would also like to thank E. Bernard, A. Gishlick and A. Millhouse for opening the fish fossils access in the Natural History Museum in London, UK; in the American Museum of Natural History in NYC, United States; and in the Smithsonian National History Museum of the Natural History in Washington, D. C., United States, respectively. Many thanks to H. Botella and C. Martínez-Pérez (University of Valencia, Spain) for scanning the Lithuanian fossils using a synchrotron in Switzerland and for sharing their experience of tomography and how to create 3D models using Avizo 8.1 software. A.S. and S.R. thank the Research Council of Lithuania (grant no. S-MIP-19-15).

References

Abel, R. L., Laurini, C. R., & Richter, M. (2012). A palaeobiologist's guide to'virtual'micro-CT preparation. *Palaeontologia Electronica, 15*(2), 1–16.

Agassiz, L. (1833–1844) Recherches sur les poisons fossils. *Imprimerie de Petitpierre, Neuchâtel*. 5:1420.

Agassiz, L. (1838). Recherches sur les poissons fossiles part III. *Petitpierre, Neuchatel et Soleure*. pp. 139–149.

Aldinger, H. (1937). Permische ganoidfische aus Ostgrönland. *Reitzels Forlag, 102*, 1–392.

Andreev, P. S. (2011). Convergence in dental histology between the Late Triassic semionotiform *Sargodon tomicus* (Neopterygii)

and a Late Cretaceous (Turonian) pycnodontid (Neopterygii: Pycnodontiformes) species. *Microscopy Research and Technique, 74*, 464–479.

Arratia, G., Kriwet, J., & Heinrich, W. D. (2002). Selachians and actinopterygians from the Upper Jurassic of Tendaguru, Tanzania. *Fossil Record, 5*, 207–230.

Becker, F., & Bechstädt, T. (2006). Sequence stratigraphy of a carbonate-evaporite succession (Zechstein 1, Hessian Basin, Germany). *Sedimentology,53*(5), 1083–1120.

Bendix-Almgreen, S. E. (1975) Fossil fishes from the marine late Palaeozoic of Holm Land-Amdrup Land, North-East Greenland (Vol. 195, No. 9). [Nyt Nordisk Forlag]: CA, Reitzel.

Błażejowski, B. (2004). Shark teeth from the Lower Triassic of Spitsbergen and their histology. *Polish Polar Research, 25*(2), 153–167.

Bonaparte, C. L. (1832–1831) Iconographia della fauna Italica per le quattro classi degli animali vertebrati. 3. Rome

Böttinger, M., Meier-Fleischer, K., Ulmen, C. (2013) Tutorial: interactive 3D visualization in earth system research with Avizo Green 8.0. DKRZ/KlimaCampus Hamburg. p.135

Casier, E. (1959). Contributions à l'étude des poissons fossiles de la Belgique. XII—Sélaciens et Holocéphales sinémuriens de la Province de Luxembourg. *Bulletin de l'Institut Royal des Sciences Naturelles de Belgique, 38*(8), 1–35. **(French)**.

Cavin, L., Deesri, U., & Suteethorn, V. (2009). The Jurassic and Cretaceous bony fish record (Actinopterygii, Dipnoi) from Thailand. *Geological Society London Special Publications, 315*, 125–139.

Chen, D., Janvier, P., Ahlberg, P. E., & Blom, H. (2012). Scale morphology and squamation of the Late Silurian osteichthyan *Andreolepis* from Gotland, Sweden. *Historical Biology, 24*, 411–423.

Chen, L., Cuny, G., & Wang, X. (2007). The chondrichthyan fauna from the Middle-Late Triassic of Guanling (Guizhou province, SW China). *Historical Biology, 19*(4), 291–300.

Cope, E. D. (1887). Zittel's manual of paleontology. *American Naturalist, 17*, 1014–1019.

Cuny, G., Cobbett, A. M., Meunier, F. J., & Benton, M. J. (2010). Vertebrate microremains from the Early Cretaceous of southern Tunisia. *Geobios, 43*, 615–628.

Cuny, G., Liard, R., Deesri, U., Liard, T., Khamha, S., & Suteethorn, V. (2014). Shark faunas from the Late Jurassic—Early Cretaceous of northeastern Thailand. *Paläontologische Zeitschrift, 88*, 309–328.

Dankina, D., Chahud, A., Radzevičius, S., & Spiridonov, A. (2017). The first microfossil recors of ichthyofauna from the Naujoji Akmenė Formation (Lopingian), Karpėnai Quarry, northern Lithuania. *Geological Quarterly, 61*, 602–610.

Diedrich, C. G. (2009). A coelacanthid-rich site at Hasbergen (NW Germany): taphonomy and palaeoenvironment of a first systematic excavation in the Kupferschiefer (Upper Permian, Lopingian). *Palaeobiodiversity and Palaeoenvironments, 89*, 67–94.

Gailīte, L. I., Kuršs, V., Lukševiča, L., Lukševičs, E., Pomeranceva, R., Savaitova, L., et al. (2000). *Legends for geological maps of Latvian bedrock* (p. 101). Riga: State Geological Survey.

Gillis, J. A., & Donoghue, P. C. (2007). The homology and phylogeny of chondrichthyan tooth enameloid. *Journal of Morphology, 268*(1), 33–49.

Ginter, M., Hampe, O., Duffin, C. J., Schultze, H. P. (2010) Handbook of Paleoichthyology. Volume 3D. Chondrichthyes. Paleozoic Elasmobranchii: Teeth. Verlag Dr. Friedrich Pfeil, München pp. 168

Glikman, L. S. (1964). Class Chondrichthyes, subclass Elasmobranchii. *Osnovy Paleontologii*, *11*, 195–236.

Goto, M., Okura, M., & Ogawa, H. (1988). On teeth and dermal teeth of chondrichthyes from the Akasaka Limestone (Middle Permian), Cen− tral Japan. *Earth Science (Chikyu Kagaku), 42*, 290–297.

Hamel, M. H. (2005). A new lower actinopterygian from the early Permian of the Paraná Basin Brazil. *Journal of Vertebrate Paleontology, 25*(1), 19–26.

Hampe, O., Hairapetian, V., Dorka, M., Witzmann, F., Akbari, A. M., & Korn, D. (2013). A first late Permian fish fauna from Baghuk Mountain (Neo-Tethyan shelf, central Iran). *Bulletin of Geosciences, 88*(1), 1–20.

Hay, O. P. (1902). Bibliography and catalogue of the fossil vertebrata of North America. *Bulletin of the United States Geological Survey, 1*, 868.

Huxley, T. H. (1880). On the application of the laws of evolution to the arrangement of the Vertebrata and more particularly of the Mammalia. In: Proceedings of the Zoological Society of London 649–662

Ivanov, A. O., Nestell, G. P., & Nestell, M. K. (2013). Fish assemblage from the Capitanian (Middle Permian) of Theapache Mountains, West Texas, USA. *The Carboniferous-Permian Transition, 60*, 152–160.

Ivanov, A. O., Nilov, S. P. (2016). Microtomographic research of the vascularization system in the teeth of Palaeozoic sharks. In: Bruker microCT User Meeting

Jeppsson, L., Anehus, R., & Fredholm, D. (1999). The optimal acetate buffered acetic acid technique for extracting phosphatic fossils. *Journal of Paleontology, 73*(5), 964–972.

Johns, M. J. (1996). Diagnostic pedicle features of Middle and Late Triassic elasmobranch scales from northeastern British Columbia Canada. *Micropaleontology, 1*, 335–350.

Johnson, G. D. (1981). Hybodontoidei (Chondrichthyes) from the Wichita-Albany Group (Early Permian) of Texas. *Journal of Vertebrate Paleontology, 1*(1), 1–41.

Kazmierczak, J. O. (1967). Morphology and palaeoecology of the Productid *horridonia horrida* (Sowerby) from Zechstein of Poland. *Acta Palaeontologica Polonica, 12*(2), 239–264.

Kendall, A. C. (1984). Evaporites. In R. G. Walker (Ed.), *Facies models* (1st ed., Vol. 2, pp. 259–296). Canada: Geoscience Canada.

King, W. (1850). *The Permian fossils of England* (pp. 1–253). London: Monograph of the Palaeontographical Society.

Knoll, F., Cuny, G., Mojon, P. O., López-Antoñanzas, R., & Huguet, D. (2013). A new vertebrate-, ostracod-, and charophyte-bearing locality in the Middle Jurassic of the Grands Causses (southern France). *Proceedings of the Geologists' Association, 124*(3), 525–529.

Koot, M. B. (2013). Effects of the Late Permian mass extinction on chondrichthyan palaeobiodiversity and distribution patterns. Ph.D. dissertation, University of Plymouth, Plymouth, England (pp.859)

Koot, M. B., Cuny, G., Tintori, A., & Twitchett, R. J. (2013). A new diverse shark fauna from the Wordian (Middle Permian) Khuff Formation in the interior Haushi-Huqf area Sultanate of Oman. *Palaeontology, 56*(2), 303–343.

Koot, M. B., Gilles, C., Orchard, M. J., Richoz, S., Hart, M. B., & Twitchett, R. J. (2015). New hybodontiform and neoselachian sharks from the Lower Triassic of Oman. *Journal of Systematic Palaeontology, 13*(10), 891–917.

Kriwet, J., & Schmitz, L. (2005). New insight into the distribution and palaeobiology of the pycnodont fish Gyrodus. *Acta Palaeontologica Polonica, 50*(1), 49–56.

Kuršs, V., Savvaitova, L. (1986). *Permian limestones of Latvia*(pp. 94) Zinatne, Riga, Latvia [Russian]

Kuršs, V., Stinkule, A. (1997). *Mineral deposits of Latvia* (p. 200). Riga: University of Latvia (in Latvian)

Lukševičs, E., Stinkulis, Ģ., Mūrnieks, A., Popovs, K. (2012). Geological evolution of the Baltic Artesian Basin. In A. Dēliņa et al. (Eds.), *Highlights of groundwater research in the Baltic Artesian Basin* (pp 7–52). University of Latvia.

Magaritz, M. (1987). A new explanation for cyclic deposition in marine evaporite basins: meteoric water input. *Chemical geology, 62*(3–4), 239–250.

Manzanares, E., Pla, C., Ferrón, H. G., & Botella, H. (2018). Middle-Late Triassic chondrichthyans remains from the Betic Range (Spain). *Journal of Iberian Geology, 44*(1), 129–138.

Manzanares, E., Plá, C., Martínez-Pérez, C., Rasskin, D., & Botella, H. (2014). The enameloid microstructure of euselachian (Chondrichthyes) scales. *Paleontological Journal, 48*(10), 1060–1066.

Meyer, K. M., & Kump, L. R. (2008). Oceanic euxinia in Earth history: causes and consequences. *Annual Review of Earth and Planetary Sciences, 36*, 251–288.

Nielsen, E. (1932). Permo-Carboniferous fishes from east Greenland. *Meddelelser om Greenland, 86*(3), 1–63.

Nielsen, E. (1952). *On new or little known Edestidae from the Permian and Triassic of East Greenland* (p. 55). De danske ekspeditioner til Ostgronland: København.

Obruchev, D. V., & Orlov, Y. A. (1964). Subclass Holocephali. *Holocephalans. Fundamentals of palaeontology* (pp. 238–266). Moscow: Agnathans Fishes, Nauka Publishers.

Örvig, T. (1969). Thelodont scales from the Grey Hoek Formation of Andrée Land Spitsbergen. *Norsk Geologisk Tidsskrift, 49*(4), 387–401.

Paškevičius, J. (1997). *The Geology of the Baltic Republics* (p. 387). Vilnius.: Vilnius University and Geological Survey of Lithuania.

Patterson, C. (1965). The phylogeny of the chimaeroids. *Philosophical Transactions of the Royal Society of London, B249*, 101–219.

Patterson, C. (1966). British Wealden Sharks. *Bulletin of the British Museum (Natural History), 11*, 283–350.

Peryt, T. M., & Scholle, P. A. (1996). Regional setting and role of meteoric water in dolomite formation and diagenesis in an evaporite basin: studies in the Zechstein (Permian) deposits of Poland. *Sedimentology, 43*(6), 1005–1023.

Qu, Q., Blom, H., Sanchez, S., & Ahlberg, P. (2015). Three-dimensional virtual histology of silurian osteostracan scales revealed by synchrotron radiation microtomography. *Journal of Morphology, 276*(8), 873–888.

Raczyński, P., & Biernacka, J. (2014). Zechstein in Lithuanian-Latvian Border Region. *Geologija, 56*(2), 57–62.

Reif, W. E. (1978). Types of morphogenesis of the dermal skeleton in fossil sharks. *Paläontologische Zeitschrift, 52*, 110–128.

Richter, M. (2007). First record of Eugeneodontiformes (Chondrichthyes: Elasmobranchii) from the Paraná Basin, Late Permian of Brazil. *Paleontologia: cenários de vida. Interciéncía Ltda. Rio de Janeiro, 1*, 149–156.

Romano, C., Koot, M. B., Kogan, I., Brayard, A., Minikh, A. V., Brinkmann, W., et al. (2016). Permian-Triassic Osteichthyes (bony fishes): diversity dynamics and body size evolution. *Biological Reviews, 91*(1), 106–147.

Sallan, L. C., & Coates, M. I. (2010). End-Devonian extinction and a bottleneck in the early evolution of modern jawed vertebrates. *Proceedings of the National Academy of Sciences, 107*(22), 10131–10135.

Saravia, P. D. (2001). Upper Carboniferous fish micro-reimains from western Argentina. *Revista española de micropaleontología, 33*(2), 123–134.

Schaumberg, G. (1982). Hopleacanthus richelsdorfensis ngn sp., ein Euselachier aus dem permischen Kupferschiefer von Hessen (W-Deutschland). *Paläontologische Zeitschrift, 56*(3–4), 235–257.

Schaumberg, G. (1999). Ergänzungen zur Revision des Euselachiers *Wodnika striatula* Muenster, 1843 aus dem oberpermischen Kupferschiefer und Marl-Slate. *Geologica et Palaeontologica, 33*, 203–217.

Schindler, T. (1993). *'Elonichthys'* palatinus n. sp., a new species of actinopterygians from the Lower Permian of the Saar-Nahe Basin (SW-Germany) New Research on Permo-Carboniferous Faunas. *Pollichia-Buch, 29*, 67–81.

Shimada, K., Williamson, T. E., & Sealey, P. L. (2010). A new gigantic pycnodont fish from the Juana Lopez Member of the Upper Cretaceous Mancos Shale of New Mexico, USA. *Journal of Vertebrate Paleontology, 30*(2), 598–603.

Smith, D. B. (1979). Rapid marine transgressions and regressions of the Upper Permian Zechstein Sea. *Journal of the Geological Society, 136*(2), 155–156.

Sørensen, A. M., Håkansson, E., & Stemmerik, L. (2007). Faunal migration into the Late Permian Zechstein Basin-Evidence from bryozoan palaeobiogeography. *Palaeogeography, Palaeoclimatology, Palaeoecology, 251*(2), 198–209.

Stahl, B. J. (1999). Chondrichthyes III: Holocephali: Handbook of Paleoichthyology

Štamberg, S. (2010). A new aeduellid actinopterygian from the Lower Permian of the Krkonoše Piedmont Basin (Bohemian Massif) and its relationship to other Aeduellidae. *Bulletin of Geosciences, 85*(2), 183–198.

Štamberg, S. (2016). Actinopterygians of the Stephanian sediments of the Krkonoše Piedmont Basin (Bohemian Massif) and their palaeobiogeographic relationship. *Bulletin of Geosciences, 91*(1), 169–186.

Sweetman, S. C., Goedert, J., & Martill, D. M. (2014). A preliminary account of the fishes of the Lower Cretaceous Wessex Formation (Wealden Group, Barremian) of the Isle of Wight, southern England. *Biological journal of the Linnean Society, 113*(3), 872–896.

Szabó, M., Gulyás, P., & Ősi, A. (2016). Late Cretaceous (Santonian) pycnodontid (Actinopterygii, Pycnodontidae) remains from the freshwater deposits of the Csehbánya Formation (Iharkút, Bakony Mountains, Hungary). *Annales de Paléontologie, 2*, 123–134.

Teichert, C. (1943). Bradyodont sharks in the Permian of Western Australia. *American Journal of Science, 241*(9), 543–552.

Van Wees, J. D., Stephenson, R. A., Ziegler, P. A., Bayer, U., McCann, T., Dadlez, R., et al. (2000). On the origin of the southern Permian Basin, Central Europe. *Marine and Petroleum Geology, 17*(1), 43–59.

Weissflog, L., Elansky, N. F., Kotte, K., Keppler, F., Pfennigsdorff, A., Lange, C. A., et al. (2009). Late permian changes in conditions of the atmosphere and environments caused by halogenated gases. *Doklady Earth Sciences, 425*, 291–295.

Westoll, T. S. (1941). The Permian fishes *Dorypterus* and *Lekanichthys*. *Proceedings of the Zoological Society of London, Series B, 111*, 39–58.

Wignall, P. B. (2015). *The Worst of Times: How Life on Earth Survived Eighty Million Years of Extinctions*. Princeton: Princeton University Press.

Woodward, A. S. (1891). *Catalogue of the fossil fishes in the British Museum (Natural History), 2*. London: British Museum (Natural History).

Würdig Maciel, N. L. (1975). Ichtiodontes e Ichitiodorulitos (Pisces) da Formação Estrada Nova e Sua Aplicação na Estratigrafia do Grupo Passa Dois. *Pesquisas em Geociências, 5*(5), 7–166.

Zeeh, S., Becker, F., & Heggemann, H. (2000). Dedolomitization by meteoric fluids: the Korbach fissure of the Hessian Zechstein basin, Germany. *Journal of Geochemical Exploration, 69*, 173–176.